

HIV-1 REPLICATION AND ARHGDI5

9

9. Zhang B, Zhang Y, Dagher MC, and Shacter E: Rho GDP dissociation inhibitor protects cancer cells against drug-induced apoptosis. *Cancer Res* 2005;65(14):6054–6062.
10. Kolesnitchenko V, King L, Riva A, Tani Y, Korsmeyer SJ, and Cohen DI: A major human immunodeficiency virus type 1-initiated killing pathway distinct from apoptosis. *J Virol* 1997;71(12):9753–9763.
11. DerMardirossian C and Bokoch GM: GDIs: Central regulatory molecules in Rho GTPase activation. *Trends Cell Biol* 2005;15(7):356–363.
12. Dovas A and Couchman JR: RhoGDI: Multiple functions in the regulation of Rho family GTPase activities. *Biochem J* 2005;390(Pt 1):1–9.
13. Heasman SJ and Ridley AJ: Mammalian Rho GTPases: New insights into their functions from in vivo studies. *Nat Rev Mol Cell Biol* 2008;9(9):690–701.
14. Ladwein M and Rottner K: On the Rho'd: The regulation of membrane protrusions by Rho-GTPases. *FEBS Lett* 2008;582(14):2066–2074.
15. Brass AL, Dykxhoorn DM, Benita Y, *et al.*: Identification of host proteins required for HIV infection through a functional genomic screen. *Science* 2008;319(5865):921–926.
16. Zhou H, Xu M, Huang Q, *et al.*: Genome-scale RNAi screen for host factors required for HIV replication. *Cell Host Microbe* 2008;4(5):495–504.
17. Simmons A, Gangadharan B, Hodges A, *et al.*: Nef-mediated lipid raft exclusion of Ubch7 inhibits Cbl activity in T cells to positively regulate signaling. *Immunity* 2005;23(6):621–634.
18. Hodges A, Sharrocks K, Edelmann M, *et al.*: Activation of the lectin DC-SIGN induces an immature dendritic cell phenotype triggering Rho-GTPase activity required for HIV-1 replication. *Nat Immunol* 2007;8(6):569–577.
19. Urano E, Ichikawa R, Morikawa Y, Yoshida T, Koyanagi Y, and Komano J: T cell-based functional cDNA library screening identified SEC14-like 1a carboxy-terminal domain as a negative regulator of human immunodeficiency virus replication. *Vaccine* 2010;28(Suppl 2):B68–B74.
20. Urano E, Kariya Y, Futahashi Y, *et al.*: Identification of the P-TEFb complex-interacting domain of Brd4 as an inhibitor of HIV-1 replication by functional cDNA library screening in MT-4 cells. *FEBS Lett* 2008;582(29):4053–4058.
21. Komano J, Miyauchi K, Matsuda Z, and Yamamoto N: Inhibiting the Arp2/3 complex limits infection of both intracellular mature vaccinia virus and primate lentiviruses. *Mol Biol Cell* 2004;15(12):5197–5207.
22. Kimura K, Tsuji T, Takada Y, Miki T, and Narumiya S: Accumulation of GTP-bound RhoA during cytokinesis and a critical role of ECT2 in this accumulation. *J Biol Chem* 2000;275(23):17233–17236.
23. Takahashi Y, Tanaka Y, Yamashita A, Koyanagi Y, Nakamura M, and Yamamoto N: OX40 stimulation by gp34/OX40 ligand enhances productive human immunodeficiency virus type 1 infection. *J Virol* 2001;75(15):6748–6757.
24. Vicente-Manzanares M, Viton M, and Sanchez-Madrid F: Measurement of the levels of polymerized actin (F-actin) in chemokine-stimulated lymphocytes and GFP-coupled cDNA transfected lymphoid cells by flow cytometry. *Methods Mol Biol* 2004;239:53–68.
25. Shimizu S, Urano E, Futahashi Y, *et al.*: Inhibiting lentiviral replication by HEXIMI1, a cellular negative regulator of the CDK9/cyclin T complex. *AIDS* 2007;21(5):575–582.
26. Sato K, Aoki J, Misawa N, *et al.*: Modulation of human immunodeficiency virus type 1 infectivity through incorporation of tetraspanin proteins. *J Virol* 2008;82(2):1021–1033.
27. Togawa A, Miyoshi J, Ishizaki H, *et al.*: Progressive impairment of kidneys and reproductive organs in mice lacking Rho GDIalpha. *Oncogene* 1999;18(39):5373–5380.
28. Reif K and Cantrell DA: Networking Rho family GTPases in lymphocytes. *Immunity* 1998;8(4):395–401.
29. Tuosto L, Michel F, and Acuto O: p95vav associates with tyrosine-phosphorylated SLP-76 in antigen-stimulated T cells. *J Exp Med* 1996;184(3):1161–1166.
30. Stowers L, Yelon D, Berg LJ, and Chant J: Regulation of the polarization of T cells toward antigen-presenting cells by Ras-related GTPase CDC42. *Proc Natl Acad Sci USA* 1995;92(11):5027–5031.
31. Boulter E, Garcia-Mata R, Guilly C, *et al.*: Regulation of Rho GTPase crosstalk, degradation and activity by RhoGDI1. *Nat Cell Biol* 2010;12(5):477–483.
32. Etienne-Manneville S and Hall A: Rho GTPases in cell biology. *Nature* 2002;420(6916):629–635.
33. Dransart E, Morin A, Cherfils J, and Olofsson B: RhoGDI-3, a promising system to investigate the regulatory function of rhoGDIs: uncoupling of inhibitory and shuttling functions of rhoGDIs. *Biochem Soc Trans* 2005;33(Pt 4):623–626.
34. Lee SH and Dominguez R: Regulation of actin cytoskeleton dynamics in cells. *Mol Cells* 2010;29(4):311–325.
35. Takaishi K, Kikuchi A, Kuroda S, Kotani K, Sasaki T, and Takai Y: Involvement of rho p21 and its inhibitory GDP/GTP exchange protein (rho GDI) in cell motility. *Mol Cell Biol* 1993;13(1):72–79.
36. Miura Y, Kikuchi A, Musha T, *et al.*: Regulation of morphology by rho p21 and its inhibitory GDP/GTP exchange protein (rho GDI) in Swiss 3T3 cells. *J Biol Chem* 1993;268(1):510–515.
37. Komuro R, Sasaki T, Takaishi K, Orita S, and Takai Y: Involvement of Rho and Rac small G proteins and Rho GDI in Ca²⁺-dependent exocytosis from PC12 cells. *Genes Cells* 1996;1(10):943–951.
38. Laguet N, Sobhian B, Casartelli N, *et al.*: SAMHD1 is the dendritic- and myeloid-cell-specific HIV-1 restriction factor counteracted by Vpx. *Retrovirology* 2011;474(7353):654–657.
39. Koning FA, Newman EN, Kim EY, Kunstman KJ, Wolinsky SM, and Malim MH: Defining APOBEC3 expression patterns in human tissues and hematopoietic cell subsets. *J Virol* 2009;83(18):9474–9485.
40. Refsland EW, Stenglein MD, Shindo K, Albin JS, Brown WL, and Harris RS: Quantitative profiling of the full APOBEC3 mRNA repertoire in lymphocytes and tissues: Implications for HIV-1 restriction. *Nucleic Acids Res* 2010;38(13):4274–4284.
41. Ridley AJ: Rho GTPases and cell migration. *J Cell Sci* 2001;114(Pt 15):2713–2722.
42. Fukata M, Nakagawa M, and Kaibuchi K: Roles of Rho-family GTPases in cell polarisation and directional migration. *Curr Opin Cell Biol* 2003;15(5):590–597.
43. Iyengar S, Hildreth JE, and Schwartz DH: Actin-dependent receptor colocalization required for human immunodeficiency virus entry into host cells. *J Virol* 1998;72(6):5251–5255.
44. Jimenez-Baranda S, Gomez-Mouton C, Rojas A, *et al.*: Filamin-A regulates actin-dependent clustering of HIV receptors. *Nat Cell Biol* 2007;9(7):838–846.
45. Malinowsky K, Luksza J, and Dittmar MT: Susceptibility to virus-cell fusion at the plasma membrane is reduced through expression of HIV gp41 cytoplasmic domains. *Virology* 2008;376(1):69–78.
46. Pontow SE, Heyden NV, Wei S, and Ratner L: Actin cytoskeletal reorganizations and coreceptor-mediated activation

- of rac during human immunodeficiency virus-induced cell fusion. *J Virol* 2004;78(13):7138–7147.
47. Harmon B and Ratner L: Induction of the Galpha(q) signaling cascade by the human immunodeficiency virus envelope is required for virus entry. *J Virol* 2008;82(18):9191–9205.
 48. Wang L, Zhang H, Solski PA, Hart MJ, Der CJ, and Su L: Modulation of HIV-1 replication by a novel RhoA effector activity. *J Immunol* 2000;164(10):5369–5374.
 49. Helms WS, Jeffrey JL, Holmes DA, Townsend MB, Clipstone NA, and Su L: Modulation of NFAT-dependent gene expression by the RhoA signaling pathway in T cells. *J Leukoc Biol* 2007;82(2):361–369.
 50. Lamaze C, Chuang TH, Terlecky LJ, Bokoch GM, and Schmid SL: Regulation of receptor-mediated endocytosis by Rho and Rac. *Nature* 1996;382(6587):177–179.
 51. Sodeik B: Unchain my heart, baby let me go—the entry and intracellular transport of HIV. *J Cell Biol* 2002;159(3):393–395.
 52. Naghavi MH and Goff SP: Retroviral proteins that interact with the host cell cytoskeleton. *Curr Opin Immunol* 2007;19(4):402–407.
 53. Haedicke J, de Los Santos K, Goff SP, and Naghavi MH: The Ezrin-radixin-moesin family member ezrin regulates stable microtubule formation and retroviral infection. *J Virol* 2008;82(9):4665–4670.
 54. Hecker C, Weise C, Schneider-Schaulies J, Holmes HC, and ter Meulen V: Specific binding of HIV-1 envelope protein gp120 to the structural membrane proteins ezrin and moesin. *Virus Res* 1997;49(2):215–223.
 55. Kubo Y, Yoshii H, Kamiyama H, *et al.*: Ezrin, Radixin, and Moesin (ERM) proteins function as pleiotropic regulators of human immunodeficiency virus type 1 infection. *Virology* 2008;375(1):130–140.
 56. Barrero-Villar M, Cabrero JR, Gordon-Alonso M, *et al.*: Moesin is required for HIV-1-induced CD4-CXCR4 interaction, F-actin redistribution, membrane fusion and viral infection in lymphocytes. *J Cell Sci* 2009;122(Pt 1):103–113.
 57. Fackler OT, Luo W, Geyer M, Alberts AS, and Peterlin BM: Activation of Vav by Nef induces cytoskeletal rearrangements and downstream effector functions. *Mol Cell* 1999; 3(6):729–739.

Address correspondence to:

Jun Komano
 AIDS Research Center
 National Institute of Infectious Diseases
 1-23-1 Toyama, Shinjuku
 Tokyo 162-8640, Japan

E-mail: ajkomano@nih.go.jp

Novel Mouse Xenograft Models Reveal a Critical Role of CD4⁺ T Cells in the Proliferation of EBV-Infected T and NK Cells

Ken-Ichi Imadome¹*, Misako Yajima¹*, Ayako Arai², Atsuko Nakazawa³, Fuyuko Kawano¹, Sayumi Ichikawa^{1,4}, Norio Shimizu⁴, Naoki Yamamoto⁵*, Tomohiro Morio⁶, Shouichi Ohga⁷, Hiroyuki Nakamura¹, Mamoru Ito⁸, Osamu Miura², Jun Komano⁵, Shigeyoshi Fujiwara¹*

1 Department of Infectious Diseases, National Research Institute for Child Health and Development, Tokyo, Japan, **2** Department of Hematology, Tokyo Medical and Dental University, Tokyo, Japan, **3** Department of Pathology, National Center for Child Health and Development, Tokyo, Japan, **4** Department of Virology, Division of Medical Science, Medical Research Institute, Tokyo Medical and Dental University, Tokyo, Japan, **5** AIDS Research Center, National Institute of Infectious Diseases, Tokyo, Japan, **6** Department of Pediatrics and Developmental Biology, Tokyo Medical and Dental University, Tokyo, Japan, **7** Department of Perinatal and Pediatric Medicine, Graduate School of Medical Sciences, Kyushu University, Fukuoka, Japan, **8** Central Institute for Experimental Animals, Kawasaki, Japan

Abstract

Epstein-Barr virus (EBV), a ubiquitous B-lymphotropic herpesvirus, ectopically infects T or NK cells to cause severe diseases of unknown pathogenesis, including chronic active EBV infection (CAEBV) and EBV-associated hemophagocytic lymphohistiocytosis (EBV-HLH). We developed xenograft models of CAEBV and EBV-HLH by transplanting patients' PBMC to immunodeficient mice of the NOD/Shi-*scid*/IL-2R γ^{null} strain. In these models, EBV-infected T, NK, or B cells proliferated systemically and reproduced histological characteristics of the two diseases. Analysis of the TCR repertoire expression revealed that identical predominant EBV-infected T-cell clones proliferated in patients and corresponding mice transplanted with their PBMC. Expression of the EBV nuclear antigen 1 (EBNA1), the latent membrane protein 1 (LMP1), and LMP2, but not EBNA2, in the engrafted cells is consistent with the latency II program of EBV gene expression known in CAEBV. High levels of human cytokines, including IL-8, IFN- γ , and RANTES, were detected in the peripheral blood of the model mice, mirroring hypercytokinemia characteristic to both CAEBV and EBV-HLH. Transplantation of individual immunophenotypic subsets isolated from patients' PBMC as well as that of various combinations of these subsets revealed a critical role of CD4⁺ T cells in the engraftment of EBV-infected T and NK cells. In accordance with this finding, *in vivo* depletion of CD4⁺ T cells by the administration of the OKT4 antibody following transplantation of PBMC prevented the engraftment of EBV-infected T and NK cells. This is the first report of animal models of CAEBV and EBV-HLH that are expected to be useful tools in the development of novel therapeutic strategies for the treatment of the diseases.

Citation: Imadome K-I, Yajima M, Arai A, Nakazawa A, Kawano F, et al. (2011) Novel Mouse Xenograft Models Reveal a Critical Role of CD4⁺ T Cells in the Proliferation of EBV-Infected T and NK Cells. *PLoS Pathog* 7(10): e1002326. doi:10.1371/journal.ppat.1002326

Editor: Shou-Jiang Gao, University of Texas Health Science Center San Antonio, United States of America

Received: January 27, 2011; **Accepted:** September 2, 2011; **Published:** October 20, 2011

Copyright: © 2011 Imadome et al. This is an open-access article distributed under the terms of the Creative Commons Attribution License, which permits unrestricted use, distribution, and reproduction in any medium, provided the original author and source are credited.

Funding: This study was supported by grants from the Ministry of Health, Labour and Welfare of Japan (H22-Nanchi-080 and H22-AIDS-002), the Grant of National Center for Child Health and Development (22A-9), a grant for the Research on Publicly Essential Drugs and Medical Devices from The Japan Health Sciences Foundation (KHC1014), and the Grant-in-Aid for Scientific Research (C) (H22-22590374). The funders had no role in study design, data collection and analysis, decision to publish, or preparation of the manuscript.

Competing Interests: The authors have declared that no competing interests exist.

* E-mail: imadome@nch.go.jp (KI); shige@nch.go.jp (SF)

‡ Current address: Department of Microbiology, Yong Loo Lin School of Medicine, National University of Singapore, Singapore

§ These authors contributed equally to this work.

Introduction

Epstein-Barr virus (EBV) is a ubiquitous γ -herpesvirus that infects more than 90% of the adult population in the world. EBV is occasionally involved in the pathogenesis of malignant tumors, such as Burkitt lymphoma, Hodgkin lymphoma, and nasopharyngeal carcinoma, along with the post-transplantation lymphoproliferative disorders in immunocompromised hosts. Although EBV infection is asymptomatic in most immunologically competent hosts, it sometimes causes infectious mononucleosis (IM), when primarily infecting adolescents and young adults [1]. EBV infects human B cells efficiently *in vitro* and transform them into lymphoblastoid cell lines (LCLs) [2]. Experimental infection of T

and NK cells, in contrast, is practically impossible except in limited conditions [3,4]. Nevertheless, EBV has been consistently demonstrated in T or NK cells proliferating monoclonally or oligoclonally in a group of diseases including chronic active EBV infection (CAEBV) and EBV-associated hemophagocytic lymphohistiocytosis (EBV-HLH) [5,6,7,8,9,10]. CAEBV, largely overlapping the systemic EBV⁺ T-cell lymphoproliferative diseases of childhood defined in the WHO classification of lymphomas [11], is characterized by prolonged or relapsing IM-like symptoms, unusual patterns of antibody responses to EBV, and elevated EBV DNA load in the peripheral blood [12,13,14]. CAEBV has a chronic time course with generally poor prognosis; without a proper treatment by hematopoietic stem cell transplantation, the

Author Summary

Epstein-Barr virus (EBV) is a ubiquitous human herpesvirus that infects more than 90% of the adult human population in the world. EBV usually infects B lymphocytes and does not produce symptoms in infected individuals, but in rare occasions it infects T or NK lymphocytes and causes severe diseases such as chronic active EBV infection (CAEBV) and EBV-associated hemophagocytic lymphohistiocytosis (EBV-HLH). We developed mouse models of these two human diseases in which EBV-infected T or NK lymphocytes proliferate in mouse tissues and reproduce human pathologic conditions such as overproduction of small proteins called “cytokines” that produce inflammatory responses in the body. These mouse models are thought to be very useful for the elucidation of the pathogenesis of CAEBV and EBV-HLH as well as for the development of therapeutic strategies for the treatment of these diseases. Experiments with the models demonstrated that a subset of lymphocytes called CD4-positive lymphocytes are essential for the proliferation of EBV-infected T and NK cells. This result implies that removal of CD4-positive lymphocytes or suppression of their functions may be an effective strategy for the treatment of CAEBV and EBV-HLH.

majority of cases eventually develop malignant lymphoma of T or NK lineages, multi-organ failure, or other life-threatening conditions. Monoclonal or oligoclonal proliferation of EBV-infected T and NK cells, an essential feature of CAEBV, implies its malignant nature, but other characteristics of CAEBV do not necessarily support this notion. For example, EBV-infected T or NK cells freshly isolated from CAEBV patients, as well as established cell lines derived from them, do not have morphological atypia and do not engraft either in nude mice or *scid* mice (Shimizu, N., unpublished results). Clinically, CAEBV has a chronic time course and patients may live for many years without progression of the disease [15]. Although patients with CAEBV do not show signs of explicit immunodeficiency, some of them present a deficiency in NK-cell activity or in EBV-specific T-cell responses, implying a role for subtle immunodeficiency in its pathogenesis [16,17,18].

EBV-HLH is the most common and the severest type of virus-associated HLH and, similar to CAEBV, characterized by monoclonal or oligoclonal proliferation of EBV-infected T (most often CD8⁺ T) cells [5,6]. Clinical features of EBV-HLH include high fever, pancytopenia, coagulation abnormalities, hepatosplenomegaly, liver dysfunction, and hemophagocytosis [19]. Overproduction of cytokines by EBV-infected T cells as well as by activated macrophages and T cells reacting to EBV is thought to play a central role in the pathogenesis [20]. Although EBV-HLH is an aggressive disease requiring intensive clinical interventions, it may be cured, in contrast to CAEBV, by proper treatment with immunomodulating drugs [21]. No appropriate animal models have been so far developed for either CAEBV or EBV-HLH.

NOD/Shi-*scid*/IL-2R γ^{null} (referred here as NOG) is a highly immunodeficient mouse strain totally lacking T, B, and NK lymphocytes, and transplantation of human hematopoietic stem cells to NOG mice results in reconstitution of human immune system components, including T, B, NK cells, dendritic cells, and macrophages [22,23]. These so called humanized mice have been utilized as animal models for the infection of certain human viruses targeting the hemato-immune system, including human immunodeficiency virus 1 (HIV-1) and EBV [24,25,26,27,28,29,30]. Xeno-

transplantation of human tumor cells to NOG mice also provided model systems for several hematologic malignancies [31,32,33]. To facilitate investigations on the pathogenesis of CAEBV and EBV-HLH and assist the development of novel therapeutic strategies, we generated mouse models of these two EBV-associated diseases by transplanting NOG mice with PBMC isolated from patients with the diseases. In these models, EBV-infected T, NK, or B cells engrafted in NOG mice and reproduced lymphoproliferative disorder similar to either CAEBV or EBV-HLH. Further experiments with the models revealed a critical role of CD4⁺ T cells in the *in vivo* proliferation of EBV-infected T and NK cells.

Results

Engraftment of EBV-infected T and NK cells in NOG mice following xenotransplantation with PBMC of CAEBV patients

Depending on the immunophenotypic subset in which EBV causes lymphoproliferation, CAEBV is classified into the T-cell and NK-cell types, with the former being further divided into the CD4, CD8, and $\gamma\delta$ T types. The nine patients with CAEBV examined in this study are characterized in Table 1 and include all these four types. Intravenous injection of $1-4 \times 10^6$ PBMC isolated from these nine patients resulted in successful engraftment of EBV-infected T or NK cells in NOG mice in a reproducible manner (Table 1). The results with the patient 1 (CD4 type), patient 3 (CD8 type), patient 5 ($\gamma\delta$ T type), and patient 9 (NK type) are shown in Figure 1. Seven to nine weeks post-transplantation, EBV DNA was detected in the peripheral blood of recipient mice and reached the levels of 10^5-10^8 copies/ μ g DNA (Figure 1A). By contrast, no engraftment of EBV-infected cells was observed when immunophenotypic fractions containing EBV DNA were isolated from PBMC and injected to NOG mice (Figure 1A and Table 2). An exception was the CD4⁺ T-cell fraction isolated from patients with the CD4 type CAEBV, that reproducibly engrafted when transplanted without other components of PBMC (Figure 1A, Table 2). Flow cytometry revealed that the major population of engrafted cells was either CD4⁺, CD8⁺, TCR $\gamma\delta$ or CD16⁺CD56⁺, depending on the type of the donor CAEBV patient (Figure 1B). EBV-infected cells of identical immunophenotypes were found in the patients and the corresponding mice that received their respective PBMC (Figure 1B). Although human cells of multiple immunophenotypes were present in most recipient mice, fractionation by magnetic beads-conjugated antibodies and subsequent real-time PCR analysis detected EBV DNA only in the predominant immunophenotypes that contained EBV DNA in the original patients (Figure 1B, Table 1). The EBV DNA load observed in individual lymphocyte subsets in the patient 3 and a mouse that received her PBMC is shown as supporting data (Table S1). When PBMC from three healthy EBV-carriers were injected intravenously to NOG mice, as controls, no EBV DNA was detected from either the peripheral blood, spleen, or liver (data not shown). Histological analyses of the spleen and the liver of these control mice identified no EBV-encoded small RNA (EBER)-positive cells, although some CD3-positive human T cells were observed (Figure S2). Analysis of TCR V β repertoire demonstrated an identical predominant T-cell clone in patients 1 and 3) and the corresponding mice that received their PBMC (Figure 1C). The general condition of most recipient mice deteriorated gradually in the observation period of eight to twelve weeks, with loss of body weight (Figure S1), ruffled hair, and inactivity.

NOG mice engrafted with EBV-infected T or NK cells were sacrificed for pathological and virological analyses between eight

Table 1. Patients with EBV-T/NK LPD and the results of xenotransplantation of their PBMC to NOG mice.

Patient number	Diagnosis	Sex	Age	Type of infected cells	¹ EBV DNA load in the patients	² Engrafted cells in mice	³ Engraftment	¹ EBV DNA load in mice
1	CAEBV	F	25	CD4	9.2×10 ⁵	<u>CD4</u> , CD8	3/3	1.0~3.8×10 ⁷
2	CAEBV	M	46	CD4	1.3~7.2×10 ⁵	<u>CD4</u> , CD8	2/2, 3/3	2.6~10×10 ⁵
3	CAEBV	F	35	CD8	2.1~78×10 ⁵	<u>CD8</u> , CD4	2/2, 2/2	1.1~33×10 ⁶
4	CAEBV	M	28	CD8	8.2×10 ⁵	<u>CD8</u> , CD4	3/3	1.1~2.5×10 ⁶
5	CAEBV	M	10	γδT	2.2×10 ⁶	<u>γδT</u> , CD4, CD8	2/2	3.8~6.5×10 ⁶
6	CAEBV	F	15	γδT	6.2×10 ⁵	<u>γδT</u> , CD4, CD8	2/2	2.2~11×10 ⁵
7	CAEBV	M	13	NK	1.1~6.7×10 ⁵	<u>NK</u> , CD4, CD8	2/2, 2/2	0.6~15×10 ⁴
8	CAEBV	F	13	NK	6.3×10 ⁶	<u>NK</u> , CD4, CD8	3/3, 2/2	0.8~1.9×10 ⁵
9	CAEBV	M	8	NK	1.2~8.7×10 ⁵	<u>NK</u> , CD4, CD8	2/2, 3/3	1.8~7.2×10 ⁵
10	EBV-HLH	M	10	CD8	2.8~38×10 ⁴	<u>CD8</u> , CD4	2/2, 2/2	6.5~9.9×10 ⁴
11	EBV-HLH	M	50	CD8	6.2×10 ⁵	<u>CD8</u> , CD4	4/4	7.0~45×10 ⁴
12	EBV-HLH	M	1	CD8	3.1×10 ⁵	<u>CD8</u> , CD4	2/2	6.0~9.1×10 ⁴
13	EBV-HLH	M	64	CD8	3.2~3.9×10 ⁵	<u>CD8</u> , CD4	2/2, 2/2	5.0~30×10 ⁵

¹EBV DNA copies/μg DNA in the peripheral blood.

²EBV DNA was detected only in the cells of the underlined subsets.

³Number of mice with successful engraftment per number of recipient mice is shown for each experiment.

doi:10.1371/journal.ppat.1002326.t001

and twelve weeks post-transplantation. On autopsy, the majority of mice presented with splenomegaly, with slight hepatomegaly in occasional cases (Figure 2A). Histopathological findings obtained from a representative mouse (recipient of PBMC from the patient 3 (CD8 type)) are shown in Figure 2B and reveal infiltration of human CD3⁺CD20⁻ cells to major organs, including the spleen, liver, lungs, kidneys, and small intestine. These cells were positive for both EBER and human CD45RO, indicating that they are EBV-infected human T cells (Figure 2B). In contrast, no EBV-infected T cells were found in mice transplanted with PBMC isolated from a normal EBV carrier (Figure S2). Histopathology of a control NOG mouse is shown in Figure S2. Morphologically, EBV-infected cells are relatively small and do not have marked atypia. The infiltration pattern was leukemic and identical with chronic active EBV infection in children [34]. The architecture of the organs was well preserved in spite of marked lymphoid infiltration. The spleen showed marked expansion of periarterial lymphatic sheath owing to lymphocytic infiltration. In the liver, a dense lymphocytic infiltration was observed in the portal area and in the sinusoid. The lung showed a picture of interstitial pneumonitis and the lymphocytes often formed nodular aggregations around bronchioles and arteries. In the kidney, dense lymphocytic infiltration caused interstitial nephritis. In the small intestine, mild lymphoid infiltration was seen in mucosa. Quantification of EBV DNA in the spleen, liver, lymph nodes, lungs, kidneys, adrenals, and small intestine of this mouse revealed EBV DNA at the levels of 1.5–5.1×10⁷ copies/μg DNA. Mice transplanted with PBMC derived from CAEBV of other types exhibited similar infiltration of EBV-infected T or NK cells to the spleen, liver, and other organs (Figure 2C and data not shown).

EBV-infected T- and NK-cell lines established from CAEBV patients do not engraft in NOG mice

We established EBV-positive cell lines of CD4⁺ T, CD8⁺ T, γδT, and CD56⁺ NK lineages from PBMC of the patients listed in Table 1 by the method described previously [35], and confirmed by flow cytometry that the surface phenotypes of EBV-infected cells in the original patients were retained in these cell lines (data

not shown). To test whether these cell lines engraft in NOG mice, 1–4×10⁶ cells were injected intravenously to NOG mice. The results are shown in Figure 3A and indicate that CAEBV-derived cell lines of the CD8⁺ T, γδT, and CD56⁺ NK phenotypes do not engraft in NOG mice. Neither human CD45-positive cells nor EBV DNA were detected in the peripheral blood of the mice up to twelve weeks post-transplantation. When the recipient mice were sacrificed at twelve weeks post-injection, no EBV DNA could be detected in the spleen, liver, bone marrow, mesenteric lymph nodes, and kidneys. In contrast, the CD4⁺ T cell lines derived from the CD4-type patients 1 and 2 engrafted in NOG mice and induced T lymphoproliferation similar to that induced by PBMC isolated freshly from these patients (Figure 3A and data not shown). These results, together with the results of transplantation with EBV-containing subsets of PBMC, indicate that EBV-infected T and NK cells, with the exception of those of the CD4⁺ subset, are not able to engraft in NOG mice, when they are separated from other components of PBMC, suggesting that some components of PBMC are essential for the outgrowth EBV-infected T and NK cells in NOG mice.

Engraftment of EBV-infected T and NK cells in NOG mice requires CD4⁺ T cells

To identify the cellular component required for the engraftment of EBV-infected T and NK cells in NOG mice, we transplanted PBMC of CAEBV patients after removing individual immunophenotypic subsets by magnetic beads-conjugated antibodies. The results are shown in Figure 3B and summarized in Table 2. With respect to the patients 3 and 4, in whom CD8⁺ T cells are infected with EBV, removal of CD8⁺ cells from PBMC, as expected, resulted in the failure of engraftment, whereas elimination of CD19⁺, CD56⁺, or CD14⁺ cells did not affect engraftment. Importantly, elimination of CD4⁺ cell fraction, that did not contain EBV DNA, resulted in the failure of engraftment of EBV-infected T cells (Figure 3B and data not shown). In the experiments with the patients 5 and 6, in whom γδT cells were infected, removal CD4⁺ cells that did not contain EBV DNA, as well as that of γδT cells, resulted in the failure of engraftment.

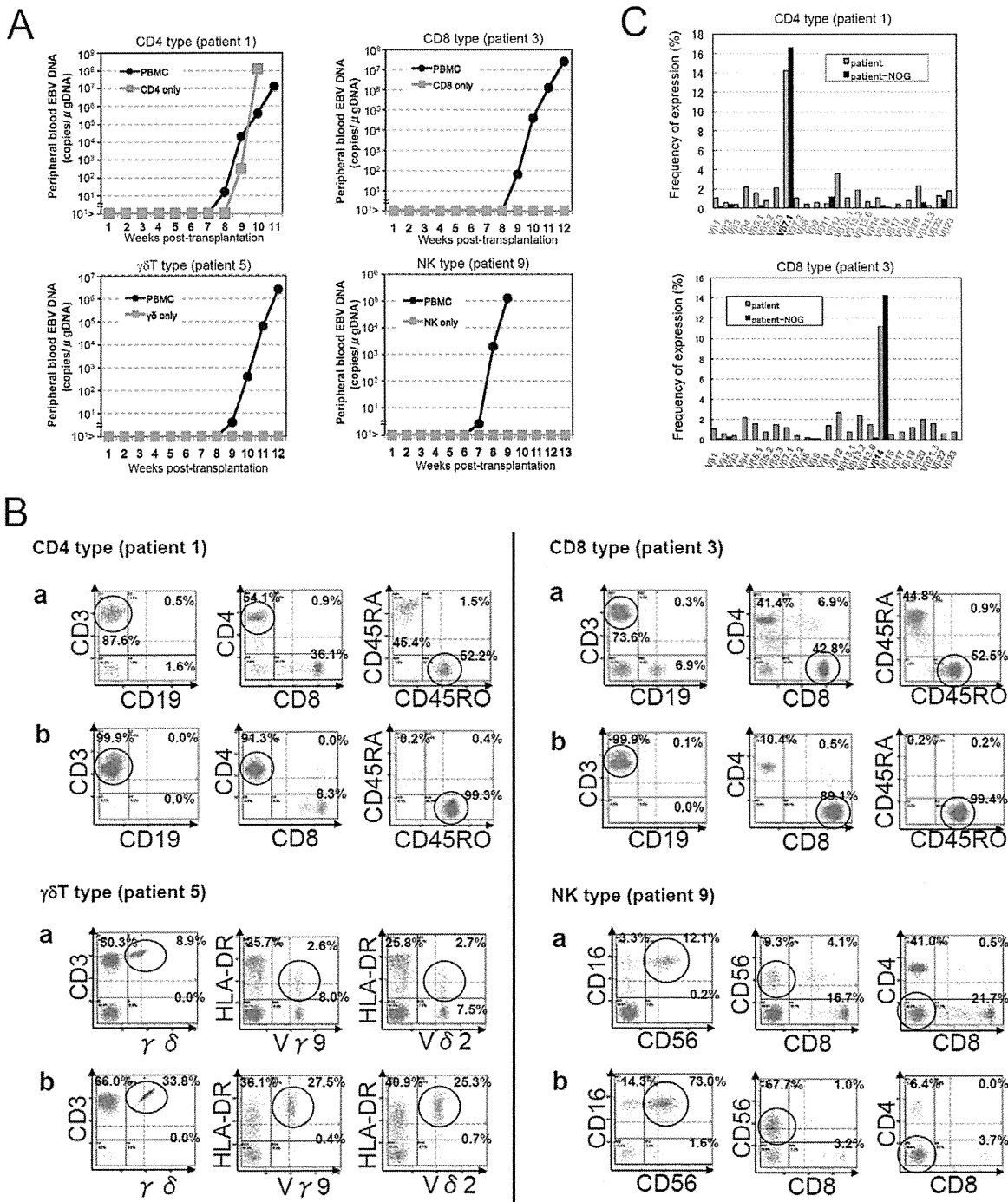


Figure 1. Engraftment of EBV-infected T or NK cells in NOG mice following transplantation with PBMC of patients with CAEBV. A. Measurement of EBV DNA levels. PBMC obtained from the CAEBV patients 1 (CD4 type), 3 (CD8 type), 5 ($\gamma\delta$ T type), and 9 (NK type) were injected intravenously to NOG mice and EBV DNA load in their peripheral blood was measured weekly by real-time PCR. The results of transplantation with whole PBMC or with isolated EBV DNA-containing cell fraction are shown. B. Flow-cytometric analysis on the expression of surface markers in the peripheral blood lymphocytes of patients (a) with CAEBV and NOG mice (b) that received PBMC from them. Human lymphocytes gated by the pattern of side scatter and human CD45 expression were further analyzed for the expression of various surface markers indicated in the figures. The results from the patients 1, 3, 5, and 9, and the corresponding mice that received their respective PBMC are shown. Circles indicate the fractions that contained EBV DNA. C. Analysis on the expression of TCR β repertoire. Peripheral blood lymphocytes obtained from the patients 1 (CD4 type) and 3 (CD8 type), and from the corresponding mice that received their respective PBMC were analyzed for the expression of β alleles. The percentages of T cells expressing each β allele are shown for the patients (grey bars) and the mice (black bars). doi:10.1371/journal.ppat.1002326.g001

Removal of CD8⁺, CD14⁺, CD19⁺, or CD56⁺ cells did not have an influence on the engraftment (Figure 3B and data not shown). Regarding the patients 8 and 9 in whom EBV resided in CD56⁺

NK cells, removal of CD4⁺ as well as CD56⁺ cells resulted in the failure of engraftment, whereas that of CD8⁺, CD19⁺, or CD14⁺ cells did not affect engraftment (Figure 3B and data not shown). In

Table 2. Results of xenotransplantation with subsets of PBMC obtained from CAEBV patients.

Number of patient	Diagnosis	Phenotype of infected cells	Cell fraction transplanted	Number of transplanted cells	Engraftment
1	CAEBV	CD4	PBMC	2×10 ⁶	+
			CD4	2×10 ⁶	+
			PBMC-CD4	3×10 ⁶	–
			PBMC-CD8	2×10 ⁶	+
			PBMC-CD56	2×10 ⁶	+
			PBMC-CD14	2×10 ⁶	+
			PBMC-CD19	2×10 ⁶	+
3	CAEBV	CD8	PBMC	2×10 ⁶	+
			CD8	3×10 ⁶	–
			PBMC-CD4	3×10 ⁶	–
			PBMC-CD8	3×10 ⁶	–
			PBMC-CD56	2×10 ⁶	+
			PBMC-CD14	2×10 ⁶	+
			PBMC-CD19	2×10 ⁶	+
5	CAEBV	γδT	PBMC	2×10 ⁶	+
			γδT	3×10 ⁶	–
			PBMC-CD4	3×10 ⁶	–
			PBMC-γδT	3×10 ⁶	–
			PBMC-CD8	3×10 ⁶	+
			PBMC-CD56	3×10 ⁶	+
			PBMC-CD14	3×10 ⁶	+
9	CAEBV	NK	PBMC	2×10 ⁶	+
			NK	3×10 ⁶	–
			PBMC-CD4	3×10 ⁶	–
			PBMC-CD8	3×10 ⁶	+
			PBMC-CD56	3×10 ⁶	–
			PBMC-CD14	3×10 ⁶	+
			PBMC-CD19	3×10 ⁶	+
11	EBV-HLH	CD8	PBMC	2×10 ⁶	+
			PBMC-CD4	4×10 ⁶	–

doi:10.1371/journal.ppat.1002326.t002

the patients 1 and 2, in whom CD4⁺ T cells were infected, only the removal of CD4⁺ cells blocked the engraftment of EBV-infected cells and depletion of either CD8⁺, CD19⁺, or CD14⁺ cells had no effect (Figure 3B and data not shown). These results suggested that EBV-infected cells of the CD8⁺, γδT, and CD56⁺ lineages require CD4⁺ cells for their engraftment in NOG mice. To confirm this interpretation, we performed complementation experiments, in which EBV-containing fractions of the CD8⁺ (patient 4), γδT (patient 5), or CD56⁺ (patient 7) phenotypes were transplanted together with autologous CD4⁺ cells. The results are shown in Figure 3A and indicate that EBV-infected CD8⁺, γδT, or CD56⁺ cells engraft in NOG mice when transplanted together with CD4⁺ cells. Similarly, when EBV-infected cell lines of the CD8⁺, γδT, and CD16⁺ lineages were injected intravenously to NOG mice together with autologous CD4⁺ cells, these cell lines engrafted to the mice (Figure 3A). Finally, to further confirm the essential role of CD4⁺ cells, we examined the effect of the OKT-4 antibody that depletes CD4⁺ cells in vivo [24]. PBMC isolated from the CAEBV patient 3 (CD8 type) and the patient 8 (NK type) were injected

intravenously to NOG mice and OKT-4 was administered intravenously for four consecutive days starting from the day of transplantation. The results are shown in Figure 4 and indicate that OKT-4 can strongly suppress the engraftment of EBV-infected T and NK cells. In the mice treated with OKT-4, no splenomegaly was observed and EBV DNA was not detected either in the peripheral blood, spleen, liver, or lungs at eight weeks post-transplantation.

Analysis on the EBV gene expression associated with T or NK lymphoproliferation in NOG mice

Previous analysis of EBV gene expression in patients with CAEBV revealed the expression of EBNA1, LMP1, and LMP2A with the involvement of the Q promoter in the EBNA genes transcription and no expression of EBNA2, being consistent with the latency II type of EBV gene expression [36,37,38]. To test whether EBV-infected T and NK cells that proliferate in NOG mice retain this type of viral gene expression, we performed RT-PCR analysis in the spleen and the liver of mice that received

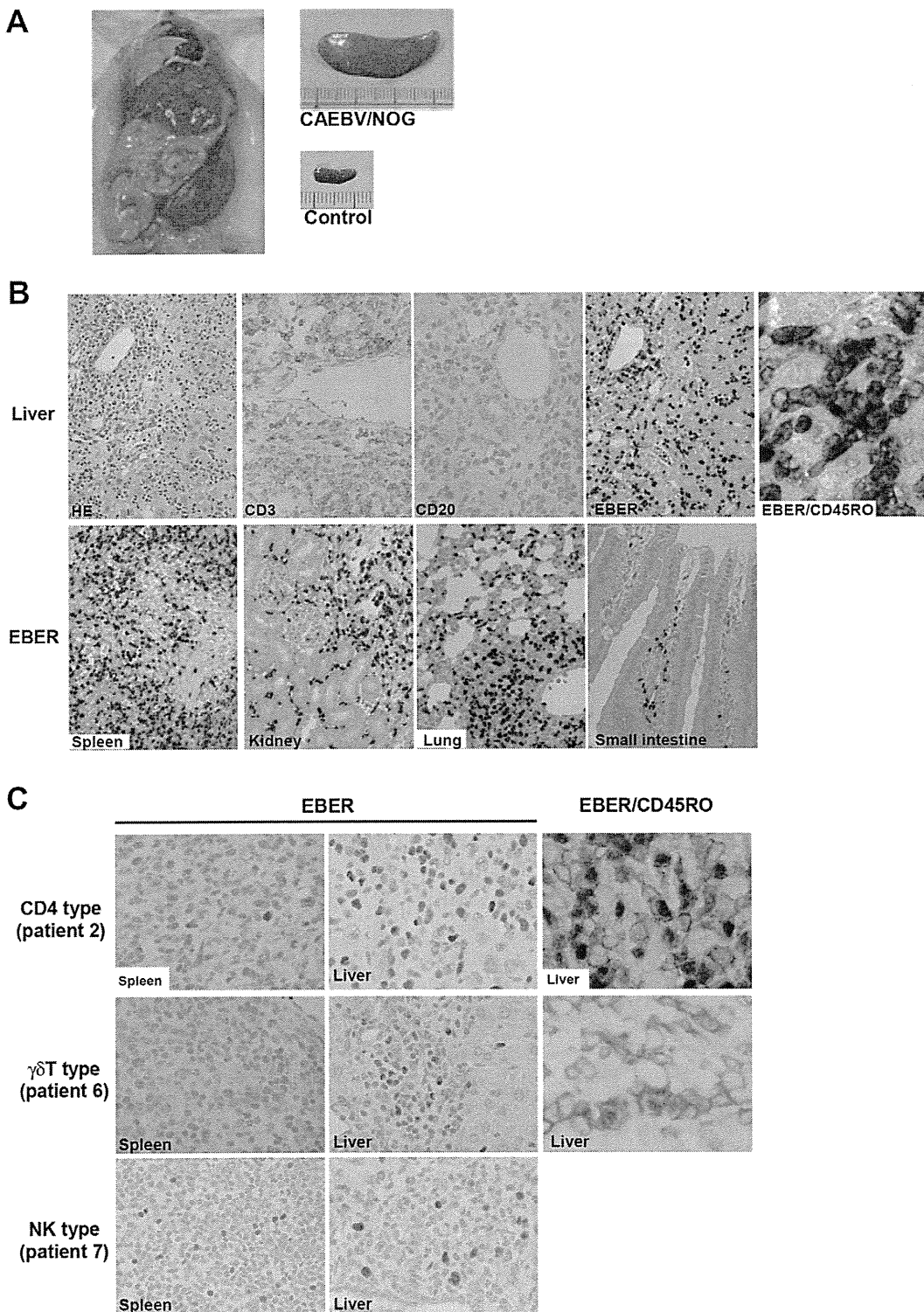


Figure 2. Pathological and immunochemical analyses on NOG mice transplanted with PBMC from CAEBV patients. A. Photographs of a model mouse showing splenomegaly and of the excised spleen. This mouse was transplanted with PBMC from the CAEBV patient 3 (CD8 type). Spleen from a control NOG mouse is also shown. B. Photomicrographs of various tissues of a mouse that received PBMC from the patient 3 (CD8 type). Upper panels: liver tissue was stained with hematoxylin-eosin (HE), antibodies specific to human CD3 or CD20, or by ISH with an EBER probe; the rightmost panel is a double staining with EBER and human CD45RO. Bottom panels: EBER ISH in the spleen, kidney, lung, and small intestine. Original magnification is $\times 200$, except for EBER/CD45RO, that is $\times 400$. C. Photomicrographs of the spleen and liver tissues obtained from NOG mice transplanted with PBMC from the CAEBV patients 2 (CD4 type), 6 ($\gamma\delta$ T type) or 7 (NK type). Tissues were stained by EBER-ISH or by double staining with EBER-ISH and human CD45RO. Original magnification $\times 600$.
doi:10.1371/journal.ppat.1002326.g002

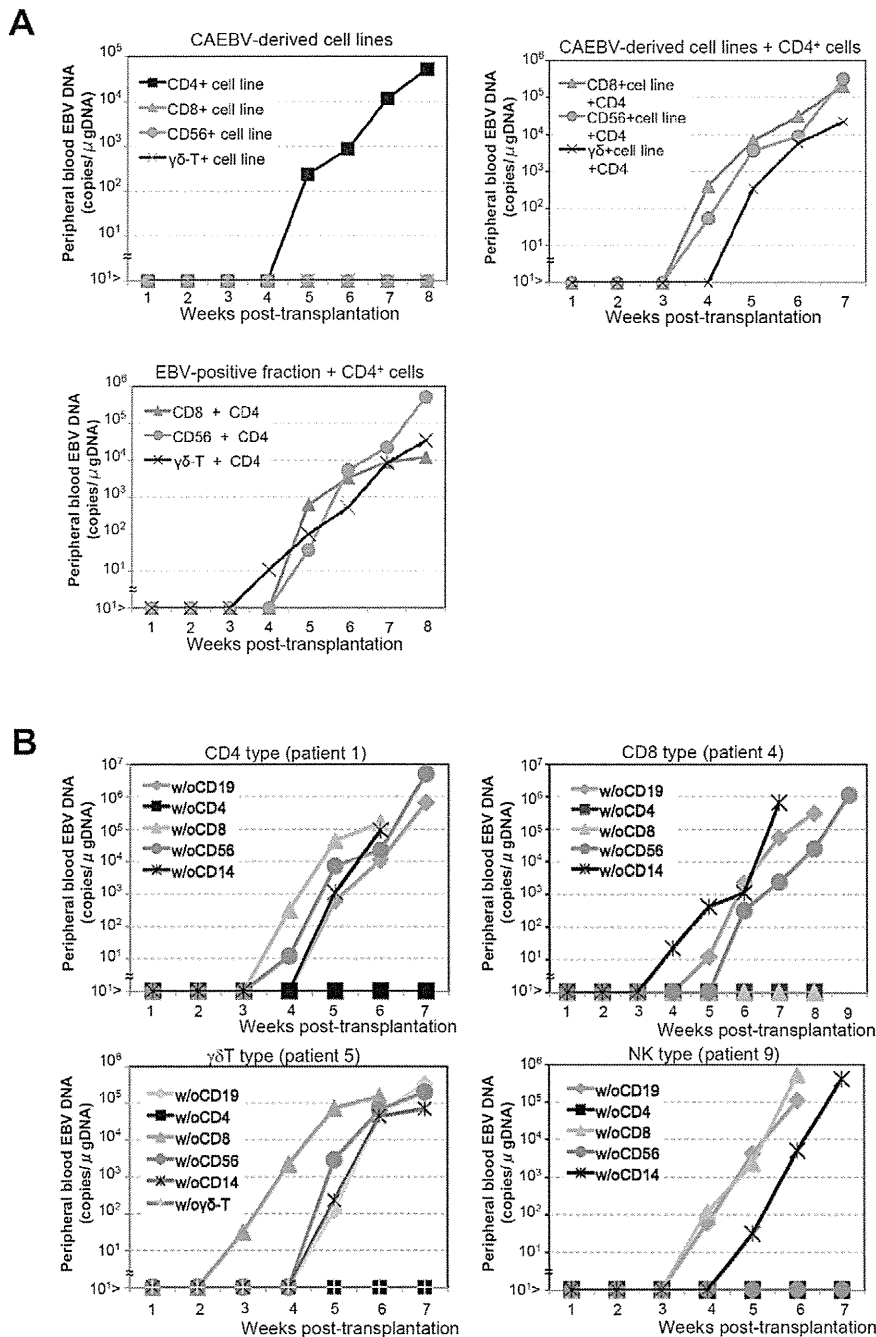


Figure 3. Analysis on the conditions of the engraftment of EBV-infected T and NK cells in NOG mice. A. EBV-infected T or NK cells isolated from patients with CAEBV or cell lines derived from them were injected to NOG mice in the conditions described below. Peripheral blood EBV DNA levels were then measured weekly. Upper-left panel: 5×10^6 cells of EBV-infected CD4⁺ T, CD8⁺ T, $\gamma\delta$ T, and CD56⁺ NK cell lines established from the CAEBV patients 1, 4, 6, and 8, respectively, were injected intravenously to NOG mice. Upper-right panel: 5×10^6 cells of the CD8⁺ T, $\gamma\delta$ T, and CD56⁺ NK cell lines established from the patients 3, 6, and 8, respectively, were injected intravenously to NOG mice together with autologous CD4⁺ T cells isolated from 5×10^6 PBMC. Bottom panel: 5×10^6 cells of the CD8⁺ T, $\gamma\delta$ T, and CD56⁺ NK fractions isolated freshly from the patients 4, 5, and 7, respectively, were injected intravenously to NOG mice together with autologous CD4⁺ T cells isolated from 5×10^6 PBMC. B. Transplantation of PBMC devoid of individual immunophenotypic subsets to NOG mice. CD19⁺, CD4⁺, CD8⁺, CD56⁺, or CD14⁺ cells were removed from PBMC obtained from the patient 1 (CD4 type, upper-left panel), 4 (CD8 type, upper-right), 5 ($\gamma\delta$ T type, bottom-left), and 9 (NK type, bottom-right) and the remaining cells were injected intravenously to NOG mice. Thereafter peripheral blood EBV DNA was determined weekly. doi:10.1371/journal.ppat.1002326.g003

PBMC from the CAEBV patient 3 (CD8 type). The results are shown in Figure 5A and demonstrate the expression of mRNAs coding for EBNA1, LMP1, LMP2A, and LMP2B, but not for EBNA2. Expression of the EBV-encoded small RNA 1 (EBER1)

was also demonstrated. EBNA1 mRNAs transcribed from either the Cp promoter or the Wp promoter were not detected, whereas those transcribed from the Q promoter was abundantly detected. These results indicate that EBV-infected T cells retain the latency

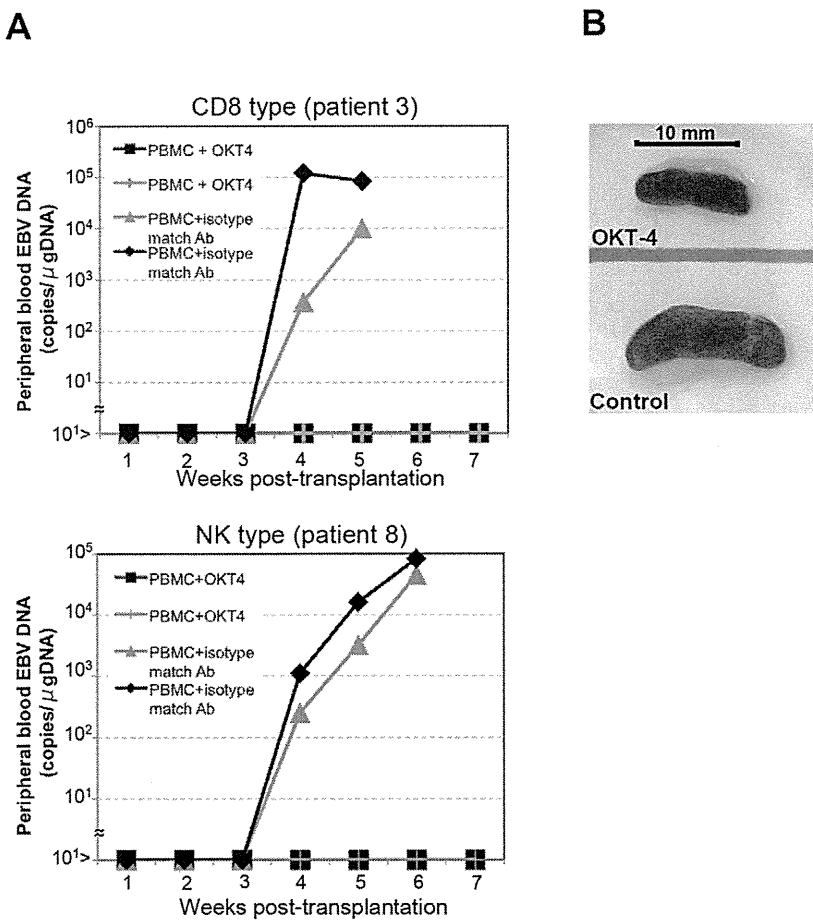


Figure 4. Suppression of the engraftment of EBV-infected T and NK cells by the OKT-4 antibody. PBMC (5×10^6 cells) isolated from the CAEBV patient 3 (CD8 type) or 8 (NK type) were injected intravenously to NOG mice. The OKT-4 antibody (100 $\mu\text{g}/\text{mouse}$) was administered intravenously on the same day of transplantation and the following three consecutive days. As a control, isotype-matched mouse IgG was injected. A. Changes in the peripheral blood EBV DNA level in the recipient mice. Results with the mice transplanted with PBMC of the patient 3 (top) and of the patient 8 (bottom) are shown. B. Photographs of the spleen of an OKT-4-treated mouse (top) and a control mouse (bottom) taken at autopsy. doi:10.1371/journal.ppat.1002326.g004

II pattern of latent EBV gene expression after engraftment in NOG mice. Similar analyses with NOG mice engrafted with EBV-infected NK cells also showed the latency II type of EBV gene expression (data not shown).

NOG mice engrafted with EBV-infected T or NK cells produce high levels of human cytokines

In patients with CAEBV, high levels of cytokines have been detected in the peripheral blood and are thought to play important roles in the pathogenesis [20,39,40]. To test whether this hypercytokinemia is reproduced in NOG mice, we examined the levels of various human cytokines in the sera of transplanted mice using ELISA kits that can quantify human cytokines specifically. The results are shown in Figure 5B and indicate that the mice transplanted with PBMC of the patient 3 (CD8 type) or the patient 8 (NK type) contained high levels of RANTES, IFN- γ , and IL-8 in their sera.

Engraftment of EBV-infected T and B cells derived from patients with EBV-HLH in NOG mice

To extend the findings obtained from the CAEBV xenograft model to another disease with EBV⁺ T/NK lymphoproliferation, we transplanted NOG mice with PBMC isolated from patients

with EBV-HLH. Characteristics of the four EBV-HLH patients examined in this study and the results of transplantation with their PBMC are summarized in Table 1. EBV DNA was detected in the peripheral blood three to four weeks post-transplantation and rapidly reached the levels of 1×10^4 to 1×10^6 copies/ μg DNA (results of typical experiments are shown in Figure 6A). Similar to the findings in CAEBV, EBV DNA was not detected in the recipient mice, when CD4⁺ cell fraction was removed from PBMC (Figure 6A). Immunophenotypic analyses on the peripheral blood lymphocytes isolated from EBV-HLH patients and corresponding recipient mice revealed that cells of an identical immunophenotype (CD3⁺CD8⁺CD45RO⁺CD19⁻CD4⁻CD45RA⁻CD16⁻CD56⁻) were present and contained EBV DNA in both the patients and corresponding mice (Figure 6C and data not shown). The EBV DNA load observed in individual lymphocyte subsets in the patient 10 and a mouse that received his PBMC is shown as supporting data (Table S2). General condition of the recipient mice deteriorated consistently more quickly, with the loss of body weight (Figure S1), ruffling of hair, and general inactivity, than those mice engrafted with EBV-infected T or NK cells derived from CAEBV. The mice were sacrificed around four weeks post-transplantation for pathological analyses. Macroscopical observation revealed moderate to severe splenomegaly (Figure 6D) in the

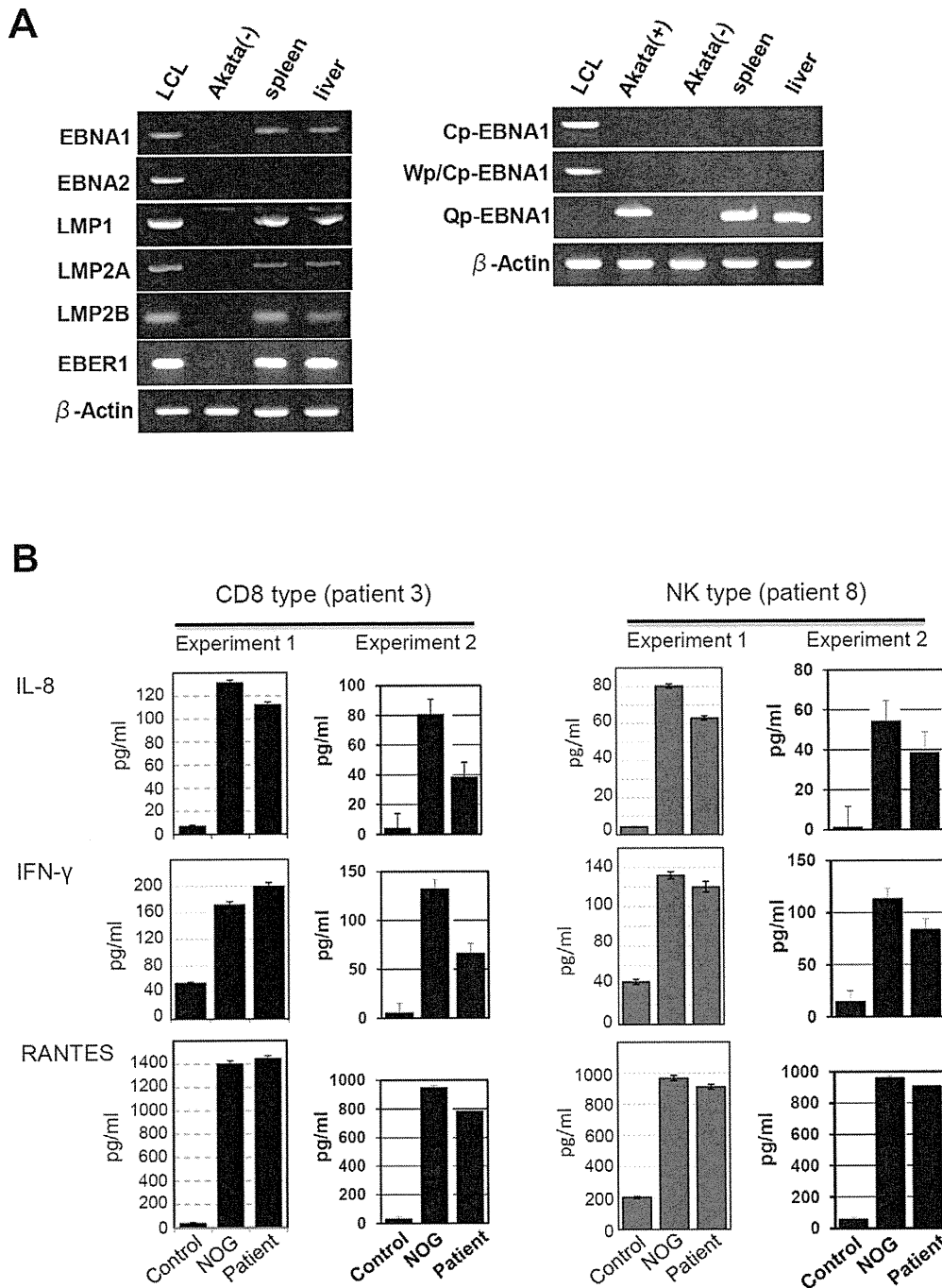


Figure 5. Analyses on the latent EBV gene expression and cytokine production in NOG mice transplanted with PBMC of CAEBV patients. A. EBV gene expression. Total RNA was purified from the spleen and liver of a mouse that received PBMC from the patient 3 (CD8 type) and applied for RT-PCR assay to detect transcripts from the indicated genes. RNA samples from an EBV-transformed B-lymphoblastoid cell line (LCL) and from EBV-negative Akata cell line were used as positive and negative controls, respectively. The primers used in the experiments are shown in Materials and Methods. B. Quantification of plasma levels of human cytokines in patients with CAEBV and corresponding recipient mice. PBMC were isolated from the patients 3 (CD8 type) and 8 (NK type) in two occasions and transplanted to NOG mice. Plasma cytokine levels of the patients were determined when their PBMC were isolated. Plasma cytokine levels of the corresponding recipient mice, prepared on each occasion of PBMC collection, were determined when they were sacrificed. Concentration of human IL-8, IFN- γ , and RANTES were measured by appropriate ELISA kits following the instruction provided by the manufacturer. Plasma samples from healthy adults were used as a control. The bars represent mean values and standard errors from triplicate measurements. doi:10.1371/journal.ppat.1002326.g005

majority of recipient mice, and slight hepatomegaly in a limited fraction of them. A finding characteristic to these mice were massive hemorrhages in the abdominal and/or thoracic cavities,

that were not seen in the mice transplanted with CAEBV-derived PBMC (Figure 6D and data not shown). These hemorrhagic lesions may reflect coagulation abnormalities characteristic to

HLH. Histopathological analyses revealed a number of EBER⁺ cells in the spleen and the liver (Figure 6E) and quantification of EBV DNA in these tissues revealed 1.4×10^1 to 2.4×10^2 copies/ μ g of EBV DNA. When the tissues were examined by immunostaining and EBER ISH, the EBER⁺ cells were shown unexpectedly to be mostly CD45RO⁻ and CD20⁺ in all five transplantation experiments with four different patients, indicating that the majority of EBV-infected cells in these tissues are of the B-cell lineage (Figure 6E and data not shown). EBER⁺ large B cells were seen scattered among numerous reactive small T cells, most of which are CD8⁺, in the tissues of the spleen, liver, lungs and kidneys. A number of macrophages were also seen in these tissues. Fractionation of mononuclear cells obtained from the liver of a mouse transplanted with PBMC of the EBV-HLH patient 10, followed by real-time PCR, detected EBV DNA (1.4×10^1 copies/ μ g DNA) only in the CD19⁺ B-cell fraction. In addition, an EBV-infected B lymphoblastoid cell line, but not an EBV-positive T cell line, could be established from this liver. Thus the presence of EBV in B cells were demonstrated by three independent methods in the tissues of EBV-HLH mice. Enzyme-linked immunosorbent assay revealed extremely high levels of human cytokines, including IL-8, IFN- γ , and RANTES, in the sera of both the original patients and the recipient mice (Figure 6B). The levels of IL-8 and IFN- γ were much higher than those observed in the peripheral blood of patients with CAEBV and mice that received their PBMC. Thus, NOG mice transplanted with EBV-HLH-derived PBMC are distinct from those transplanted with CAEBV-derived PBMC in the aggressive time course of the disease, internal hemorrhagic lesions, extremely high levels of IL-8 and IFN- γ in the peripheral blood, and the presence of EBV-infected B cells in lymphoid tissues.

Discussion

The mouse xenograft models of CAEBV and EBV-HLH developed here represent the first recapitulation of EBV-associated T/NK lymphoproliferation in experimental animals. Previously, Hayashi and others inoculated rabbits with Herpesvirus papio and succeeded in the generation of T-cell lymphoproliferative disorder with pathological findings suggestive of EBV-HLH [41]. This model, however, is based on an EBV-related virus and not EBV itself, and therefore may contain features irrelevant to the original human disease. Although the CAEBV and EBV-HLH models described here exhibited some common features, including the abundant presence of EBV-infected T or NK cells in the peripheral blood, there were some critical differences between the two models, probably reflecting the divergence of the pathophysiology of the original diseases. First of all, in the EBV-HLH model mouse, EBV was detected mainly in B cells in the spleen and the liver, while it was found mainly in T cells in the peripheral blood. This makes an obvious contrast with the CAEBV model mouse, where EBV was detected in T or NK cells in both the peripheral blood and lymphoid tissues. We do not have an explanation for the apparent discrepancy in the host cell type of EBV infection between the peripheral blood and lymphoid tissues of the EBV-HLH model. It should be, however, noted that histopathology of EBV-HLH tissues has not been fully investigated and therefore it is still possible that significant number of EBV-infected B cells are present in the lymphoid tissues of EBV-HLH patients. Other differences between the two models include much higher plasma levels of IL-8 and IFN- γ more aggressive and fatal outcome, and internal hemorrhagic lesions in EBV-HLH model mice, probably reflecting the differences in the pathophysiology of the original diseases.

EBV-positive B-cell proliferation was not seen in CAEBV model mice even in long-term observation beyond twelve weeks. This seems puzzling since low but significant amount of EBV DNA was found also in B19⁺ B-cell fraction in most patients with CAEBV. It should be noted that EBV-infected T or NK cell lines could be established relatively easily from patients with CAEBV by adding recombinant IL-2 in the medium. In contrast, establishment of EBV-infected B LCLs from these patients has been extremely difficult. In fact, we could establish B-LCLs from a few patients with CAEBV only when their PBMC were cultured on feeder cells expressing CD40 ligand. Therefore, we speculate that in the particular context of CAEBV, both in the patient and the model mouse, proliferation of EBV-infected B cells are somehow inhibited by an unknown mechanism.

Analysis on the conditions of engraftment of EBV-infected T/NK cells using these new xenograft models revealed that EBV-infected T and NK cells of the CD8⁺ T, TCR- γ δ T and CD56⁺ NK lineages and cell lines derived from them require CD4⁺ T cells for their engraftment in NOG mice. Only those EBV-infected cells and cell lines of the CD4⁺ T lineage could engraft in NOG mice on their own. These findings suggest that some factor(s) provided by CD4⁺ cells are essential for engraftment. Soluble factors produced by CD4⁺ T cells may be responsible for this function and we are currently examining cytokines, including IL-2, for their ability to support the engraftment of EBV-infected T and NK cells. It is also possible that cell to cell contact involving CD4⁺ cells is critical for engraftment. This dependence on CD4⁺ cells represents an interesting consistency with the previous finding that engraftment of EBV-transformed B lymphoblastoid cells in *scid* mice required the presence of CD4⁺ cells [42,43]. It has been speculated that T cells activated by an EBV-induced superantigen may be involved in the engraftment of EBV-infected B lymphoblastoid cells in *scid* mice [44]. Although a similar superantigen-mediated mechanism might also be assumed in T- and NK-cell lymphoproliferation in NOG mice, the data of TCR repertoire analyses (Figure 1C and data not shown) show no indication for clonal expansion of V β 13 T cells that are known to be specifically activated by the EBV-induced superantigen HERV-K18. It seems therefore unlikely that this superantigen is involved in the CD4⁺ T cell-dependent engraftment of EBV-infected T and NK cells. We expect CD4⁺ T cells and/or molecules produced by them may be an excellent target in novel therapeutic strategies for the treatment of CAEBV and EBV-HLH. In fact, administration of the OKT-4 antibody that depletes CD4⁺ cells in vivo efficiently prevented the engraftment of EBV-infected T cells. As a next step, we plan to test the effect of post-engraftment administration of OKT-4.

The dependence of EBV-infected T and NK cells on CD4⁺ T cells for their engraftment in NOG mice suggests the possibility that these cells are not capable of autonomous proliferation. Consistent with this notion, EBV-infected T and NK cell lines, including that of the CD4⁺ lineage, are dependent on IL-2 for their in vitro growth and do not engraft in either nude mice or *scid* mice when transplanted either s.c. or i.v (Shimizu, N., unpublished results). Clinically, CAEBV is a disease of chronic time course and patients carrying monoclonal EBV-infected T or NK cell population may live for many years without progression of the disease [15]. Overt malignant T or NK lymphoma usually develops only after a long course of the disease. Taking all these findings in consideration, we suppose that EBV-infected cells are not truly malignant at least in the early phase of the disease, even when they appear monoclonal. Because infection of EBV in T or NK cells is not unique to CAEBV and has been recognized also in infectious mononucleosis [45,46], the critical deficiency in

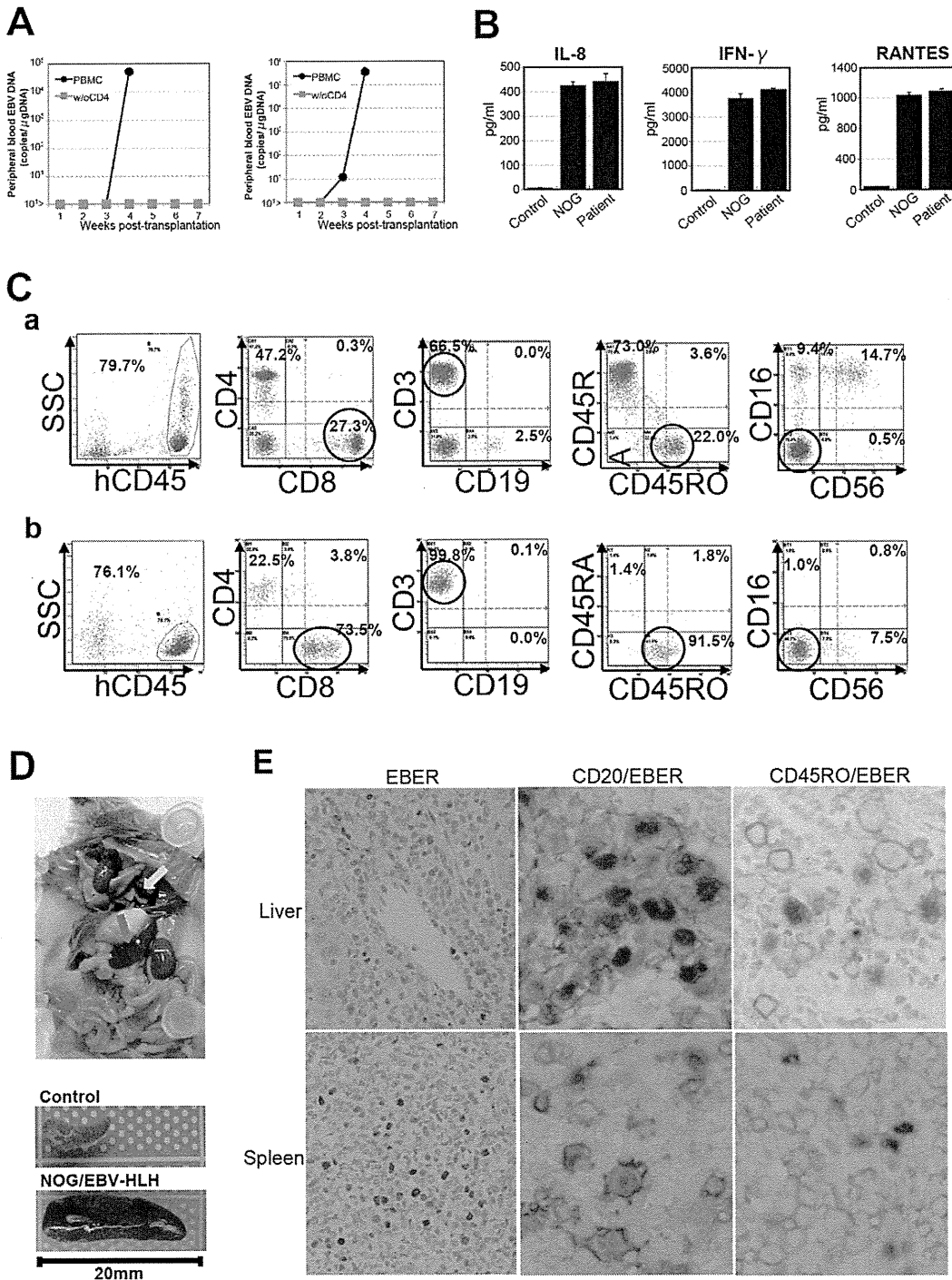


Figure 6. Engraftment of EBV-infected T and B cells in NOG mice transplanted with PBMC of patients with EBV-HLH. A. Peripheral blood EBV DNA load. Following transplantation with PBMC or PBMC devoid of CD4⁺ cells of the patient 11, EBV DNA was measured weekly by real-time PCR. Results of two mice prepared in an experiment are shown. B. Cytokine levels in the peripheral blood of the patient 12 and a mouse that received his PBMC. The levels of IL-8, IFN- γ , and RANTES were measured by ELISA in triplicates and the means and the standard errors are shown. A plasma sample of healthy person was used as a control. C. Immunophenotypic analyses on the peripheral blood lymphocytes of the EBV-HLH patient 10 (a) and a mouse that received his PBMC (b). Lymphocytes were gated by the pattern of the side scatter and the expression of human CD45, and analyzed for the expression of the indicated markers. The circles indicate the fractions that contained EBV DNA. D. Photograph of a mouse showing splenomegaly (red arrow) and hemorrhagic lesions (yellow arrow). Spleens excised from this mouse and a control mouse are shown at the bottom. E. Photomicrographs of the tissues of mice transplanted with EBV-HLH-derived PBMC. Liver and spleen tissues of a mouse transplanted with PBMC of the patient 11 were examined by EBER-ISH (left), double staining with an anti-human CD20 monoclonal antibody and EBER-ISH (middle), and double staining with an anti-human CD45RO monoclonal antibody and EBER-ISH (right). Original magnification $\times 600$.
doi:10.1371/journal.ppat.1002326.g006

CAEBV may be its inability to immunologically remove EBV-infected T and NK cells. In this context, it should be emphasized that EBV-infected T or NK cells usually exhibit the latency II pattern of EBV gene expression and do not express EBNA3s, that possess immuno-dominant epitopes recognized by EBV-specific T cells [47]. EBV-infected T and NK cells are thus not likely to be removed by cytotoxic T cells as efficiently as EBV-infected B cells that express EBNA3s. The reported lack of cytotoxic T cells specific to LMP2A [17], one of the few immuno-dominant EBV proteins expressed in the virus-infected T and NK cells, may therefore seriously affect the host's capacity to control their proliferation. A genetic defect in the perforin gene was recently identified in a patient with clinical and pathological features resembling CAEBV, suggesting that defects in genes involved in immune responses can result in clinical conditions similar to CAEBV [48].

Engraftment of EBV-infected T and NK cells in NOG mice was in most cases accompanied by co-engraftment of un-infected cell populations. These un-infected cells might have been maintained and induced to proliferate by certain factors produced by EBV-infected T or NK cells. Abundant cytokines produced by these cells may be responsible for this activity. It is also possible that the proliferation of these un-infected cells represents immune responses. Experiments are underway to test whether these un-infected T cells contain EBV-specific cells. These un-infected T cells might also be reacting to host murine tissues. Intravenous injection of PBMC obtained from normal humans to immunodeficient mice including NOG mice has been shown to induce acute or chronic graft versus host disease (GVHD) [49,50]. However, because much less PBMC were injected to mice in the present study as compared to those previous studies, it is not likely that major GVHD was induced in NOG mice transplanted with PBMC of patients with CAEBV or EBV-HLH.

CAEBV has been treated by a variety of regimens, including antiviral, cytotoxic, and immunomodulating agents with more or less unsatisfactory results. Although hematopoietic stem cell transplantation, especially that with reduced intensity conditioning can give complete remission in a substantial number of patients [51,52], it is still desirable to develop safer and more effective treatment, possibly with pharmaceutical agents. The xenograft model of CAEBV generated in this study may be an excellent animal model to test novel experimental therapies for the disease. In fact, the OKT-4 antibody that depletes CD4⁺ T cells in vivo gave a promising result implying its effectiveness as a therapeutic to CAEBV.

Materials and Methods

Ethics statement

Protocols of the experiments with materials obtained from patients with CAEBV and EBV-HLH and from control persons have been reviewed and approved by the Institutional Review Boards of the National Center for Child Health and Development and of the National Institute of Infectious diseases (NIID). Blood samples of the patients and control persons were collected after obtaining written informed consent. Protocols of the experiments with NOG mice are in accordance with the Guidelines for Animal Experimentation of the Japanese Association for Laboratory Animal Science and were approved by the Institutional Animal Care and Use Committee of NIID.

Patients with CAEBV and EBV-HLH

Characteristics of the nine patients with CAEBV and the four patients with EBV-HLH examined in this study are summarized

in Table 1. Diagnosis of CAEBV and EBV-HLH was made on the basis of the published guidelines [19,53] and confirmed by identification of EBV-infected T or NK cells in their peripheral blood by flow cytometry and real-time PCR.

NOD/Shi-*scid*/IL2R γ ^{null} (NOG) mice

Mice of the NOD/Shi-*scid*/IL-2R γ ^{null} (NOG) strain [22] were obtained from the Central Institute for Experimental Animals (Kawasaki, Japan) and maintained under specific pathogen free (SPF) conditions in the animal facility of NIID, as described [22].

Transplantation of PBMC or their subfractions to NOG mice

PBMC were isolated by centrifugation on Lymphosepar I (Immuno-Biological Laboratories (IBL)) and injected intravenously to the tail vein of NOG mice at the age of 6–8 weeks. Depending on the recovery of PBMC, 1–4 × 10⁶ cells were injected to 2 to 4 mice in a typical experiment with a blood sample. For transplantation with individual cellular fractions containing EBV DNA, CD4⁺ T cells, CD8⁺ T cells, and CD56⁺ NK cells were separated with the IMag Cell Separation Systems (BD Pharmingen) following the protocol supplied by the manufacturer. To isolate $\gamma\delta$ T cells, CD19⁺, CD4⁺, CD8⁺, CD56⁺, and CD14⁺ cells were serially removed from PBMC by the IMag Cell Separation Systems. From the remaining CD19⁻CD4⁻CD8⁻CD56⁻CD14⁻ population, CD3⁺ cells were positively selected by the same kit and defined as the $\gamma\delta$ T cell fraction. To transplant PBMC lacking individual immunophenotypic subsets, CD19⁺ CD4⁺, CD8⁺, CD56⁺ or CD14⁺ cells were removed from PBMC by the IMag Cell Separation Systems and the remaining cells were injected to mice. To prepare PBMC lacking $\gamma\delta$ T cells, CD19⁺, CD4⁺, CD8⁺, CD56⁺, and CD14⁺ cells isolated from PBMC in the process of obtaining $\gamma\delta$ T cell fraction (see above) were pooled and mixed with the CD19⁻CD4⁻CD8⁻CD56⁻CD14⁻ cells that did not react with anti-CD3 antibody. For complementation experiments, an EBV-containing cell fraction and the CD4⁺ cell fraction were isolated from a sample of PBMC as described above and the mixture of these two fractions were injected to NOG mice. The approximate numbers of injected cells are shown in Table 2.

Analysis of immunophenotypes and TCR repertoire expression by flow cytometry

PBMC isolated from the patients and the recipient NOG mice as described above were incubated for 30 min on ice with a mixture of appropriate combinations of fluorescently labeled monoclonal antibodies. After washing, five-color flow-cytometric analysis was carried out with the Cytomics FC500 analyzer (Beckman Coulter). The following directly labeled antibodies were used: phycoerythrin (PE)-conjugated antibodies to CD3, CD8, and TCR α/β , fluorescein isothiocyanate (FITC)-conjugated antibodies to CD3, CD4, CD8, CD19, TCRV γ 9, TCRV δ 2, and TCR γ/δ , and Phycoerythrin Texas Red (ECD)-conjugated antibody to CD45RO from Beckman Coulter; PE-conjugated antibodies to CD16, CD40, and CD40L, and FITC-conjugated antibody to CD56 from BD Pharmingen. TCR V β repertoire analysis was performed with the Multi-analysis TCR V β antibodies Kit (Beckman Coulter) according to the procedure recommended by the manufacturer.

Treatment of mice with the OKT-4 antibody

NOG mice were injected intravenously with 5 × 10⁶ PBMC isolated from the CAEBV patient 3 (CD8 type) or 8 (NK type) and were subsequently injected intravenously with 100 μ g of the OKT-4 antibody on the same day of transplantation. Additional

administration of the antibody was carried out by the same dose and route for the following three consecutive days. Peripheral blood EBV DNA load was then monitored every week. Mice were finally sacrificed four weeks post-transplantation and applied for pathological and virological analyses.

Quantification of EBV DNA by real time PCR and analysis of EBV gene expression by RT-PCR

Quantification of EBV DNA was carried out by real-time quantitative PCR assay based on the TaqMan system (Applied Biosystems), as described [54]. Analysis of EBV gene expression by RT-PCR was carried out as previously described with the following primers [55]. EBNA1: sense, gatgagcgttgggagagctgattctgca; antisense, tcctcgtccatggtttacac. EBNA2: sense, agaggagtggtgaagcggctc; antisense, tgacgggtttccaagactatcc. LMP1: sense, ctctccttctctctctt; antisense, caggagggtgatcatcagta. LMP2A: sense, atgactcatctcaacacata; antisense, catgttagcacaattgcaaa. LMP2B: sense, cagtgtaatctgcacaaaga; antisense, catgttagcacaattgcaaa. EBER1: sense, agcacc-tacgctgcctaga; antisense, aaaacatgaggaccaccagc. Cp-EBNA1: sense, cactacaagactacgctctccattcatc; anti sense, ttcggtctccctag-gccctg. Wp/Cp-EBNA1: sense, tcagagcggcaggatccacacaaat; anti-sense, ttcggtctccctaggccctg. Qp-EBNA1: sense, aggcgcgga-tagcgtgcgctaccgga; antisense, tcctcgtccatggtttacac. RT-PCR primers for β -actin were purchased from Takara (Osaka, Japan).

Histopathology, EBER ISH, and immunohistochemistry

Tissue samples were fixed in 10% buffered formalin, embedded in paraffin, and stained with hematoxylin and eosin. For phenotypic analysis of engrafted lymphocytes, immunostaining for CD3, CD8 (Nichirei), CD45RO, and CD20 (DAKO) was performed on paraffin sections. EBV was detected by in situ hybridization (ISH) with EBV small RNA (EBER) probe. Immunohistochemistry and ISH were performed on an automated stainer (BENCHMARK XT, Ventana Medical Systems) according to the manufacturer's recommendations. To determine the cell lineage of EBV infected cells, paraffin sections were applied to double staining with EBER ISH and immunohistochemistry. Immediately following EBER ISH, immunostaining for CD45RO or CD20 was performed. Photomicrographs was acquired with a OLYMPUS BX51 microscope equipped with 40x/0.75 and 20x/0.50 Uplan FI objective lens, a Pixera Penguin 600CL digital camera (Pixera), and Viewfinder 3.01 (Pixera) for white balance, contrast, and brightness correction.

Quantification of cytokines

The levels of human IL-8, IFN- γ , and RANTES in plasma samples were measured with the Enzyme-linked immunosorbent assay (ELISA) kit provided by R&D Systems following instructions provided by the manufacturer.

References

- Rickinson AB, Kieff ED (2007) Epstein-Barr virus. In: Knipe DM, Howley PM, eds. *Fields Virology* 5. ed. Philadelphia: Lippincott Williams and Wilkins. pp 2655–2700.
- Kieff ED, Rickinson AB (2007) Epstein-Barr virus and its replication. In: Knipe DM, Howley PM, eds. *Fields Virology*. Philadelphia: Lippincott Williams and Wilkins. pp 2603–2654.
- Fujiwara S, Ono Y (1995) Isolation of Epstein-Barr virus-infected clones of the human T-cell line MT-2: use of recombinant viruses with a positive selection marker. *J Virol* 69: 3900–3903.
- Watry D, Hedrick JA, Siervo S, Rhodes G, Lamberti JJ, et al. (1991) Infection of human thymocytes by Epstein-Barr virus. *J Exp Med* 173: 971–980.
- Kikuta H, Sakiyama Y, Matsumoto S, Oh-Ishi T, Nakano T, et al. (1993) Fatal Epstein-Barr virus-associated hemophagocytic syndrome. *Blood* 82: 3259–3264.
- Kawaguchi H, Miyashita T, Herbst H, Niedobitek G, Asada M, et al. (1993) Epstein-Barr virus-infected T lymphocytes in Epstein-Barr virus-associated hemophagocytic syndrome. *J Clin Invest* 92: 1444–1450.
- Kawa-Ha K, Ishihara S, Ninomiya T, Yumura-Yagi K, Hara J, et al. (1989) CD3-negative lymphoproliferative disease of granular lymphocytes containing Epstein-Barr viral DNA. *J Clin Invest* 84: 51–55.
- Jones JF, Shurin S, Abramovsky C, Tubbs RR, Sciotto CG, et al. (1988) T-cell lymphomas containing Epstein-Barr viral DNA in patients with chronic Epstein-Barr virus infections. *N Engl J Med* 318: 733–741.

Accession numbers

The Swiss-Prot accession numbers for the proteins described in this article are as follows: P13501 for RANTES; P10145 for IL-8; P01579 for IFN- γ ; P03211 for EBNA1; P12978 for EBNA2; P12977 for EBNA3; P03230 for LMP1; and Q66562 for LMP2. The DDBJ accession number for EBER is AJ315772.

Supporting Information

Figure S1 Changes in the body weight of NOG mice transplanted with PBMC derived from patients with CAEBV or EBV-HLH. Body weight of the five CAEBV mice shown in Figure 1A (transplanted with PBMC from the patient 1, 3, 5, and 9, and with the CD4⁺ fraction from the patient 1, respectively) and two EBV-HLH mice shown in Figure 6A (both transplanted with PBMC from the patient 11) were recorded weekly. (TIF)

Figure S2 Histopathological analysis of a control NOG mouse. A. a NOG mouse without xenograft. A 20-week old female NOG mouse was sacrificed and examined as a reference. No human cells are identified in these tissues. Upper panels: liver tissue was stained with hematoxylin-eosin (HE), antibodies specific to human CD3 or CD20, or by ISH with an EBER probe; the rightmost panel is a double staining with EBER and human CD45RO. Bottom panels: EBER ISH in the spleen, kidney, and small intestine. B. a NOG mouse transplanted with PBMC of a healthy EBV carrier. A six-week old female NOG mouse was transplanted with 5×10^6 PBMC isolated from a normal EBV-seropositive person and sacrificed at eight weeks post-transplantation for histological analysis. Liver and Spleen tissues were stained with HE, antibodies specific to human CD3 or CD20, or by ISH with an EBER probe. No EBER-positive cells were identified in these tissues. Original magnification is $\times 200$ for both A and B. (TIF)

Table S1 EBV DNA load in lymphocyte subsets of a patient with CAEBV and a corresponding mouse derived from her PBMC. (DOC)

Table S2 EBV DNA load in lymphocyte subsets of a patient with EBV-HLH and a corresponding mouse derived from his PBMC. (DOC)

Acknowledgments

We thank Kumiko Tanaka, Ken Watanabe, and Miki Katayama for technical assistance.

Author Contributions

Conceived and designed the experiments: KI MY NS NY SF. Performed the experiments: KI MY AN FK SI HN. Analyzed the data: KI MY AN SF. Contributed reagents/materials/analysis tools: AA TM SO MI OM JK. Wrote the paper: KI SF.

9. Kikuta H, Taguchi Y, Tomizawa K, Kojima K, Kawamura N, et al. (1988) Epstein-Barr virus genome-positive T lymphocytes in a boy with chronic active EBV infection associated with Kawasaki-like disease. *Nature* 333: 455–457.
10. Ishihara S, Tawa A, Yumura-Yagi K, Murata M, Hara J, et al. (1989) Clonal T-cell lymphoproliferation containing Epstein-Barr (EB) virus DNA in a patient with chronic active EB virus infection. *Jpn J Cancer Res* 80: 99–101.
11. Jaffe ES (2009) The 2008 WHO classification of lymphomas: implications for clinical practice and translational research. *Hematology Am Soc Hematol Educ Program* 2009: 523–531.
12. Okano M (2002) Overview and problematic standpoints of severe chronic active Epstein-Barr virus infection syndrome. *Crit Rev Oncol Hematol* 44: 273–282.
13. Straus SE (1992) Acute progressive Epstein-Barr virus infections. *Annu Rev Med* 43: 437–449.
14. Kimura H (2006) Pathogenesis of chronic active Epstein-Barr virus infection: is this an infectious disease, lymphoproliferative disorder, or immunodeficiency? *Rev Med Virol* 16: 251–261.
15. Kimura H, Morishima T, Kanegane H, Ohga S, Hoshino Y, et al. (2003) Prognostic factors for chronic active Epstein-Barr virus infection. *J Infect Dis* 187: 527–533.
16. Tsuge I, Morishima T, Kimura H, Kuzushima K, Matsuoka H (2001) Impaired cytotoxic T lymphocyte response to Epstein-Barr virus-infected NK cells in patients with severe chronic active EBV infection. *J Med Virol* 64: 141–148.
17. Sugaya N, Kimura H, Hara S, Hoshino Y, Kojima S, et al. (2004) Quantitative analysis of Epstein-Barr virus (EBV)-specific CD8+ T cells in patients with chronic active EBV infection. *J Infect Dis* 190: 985–988.
18. Aoukaty A, Lee IF, Wu J, Tan R (2003) Chronic active Epstein-Barr virus infection associated with low expression of leukocyte-associated immunoglobulin-like receptor-1 (LAIR-1) on natural killer cells. *J Clin Immunol* 23: 141–145.
19. Henter JL, Horne A, Arico M, Egeler RM, Filipovich AH, et al. (2007) HLH-2004: Diagnostic and therapeutic guidelines for hemophagocytic lymphohistiocytosis. *Pediatr Blood Cancer* 48: 124–131.
20. Lay JD, Tsao CJ, Chen JY, Kadin ME, Su IJ (1997) Upregulation of tumor necrosis factor-alpha gene by Epstein-Barr virus and activation of macrophages in Epstein-Barr virus-infected T cells in the pathogenesis of hemophagocytic syndrome. *J Clin Invest* 100: 1969–1979.
21. Imashuku S, Hibi S, Ohara T, Iwai A, Sako M, et al. (1999) Effective control of Epstein-Barr virus-related hemophagocytic lymphohistiocytosis with immunotherapy. *Histiocyte Society. Blood* 93: 1869–1874.
22. Ito M, Hiramatsu H, Kobayashi K, Suzue K, Kawahata M, et al. (2002) NOD/SCID/gamma(c)(null) mouse: an excellent recipient mouse model for engraftment of human cells. *Blood* 100: 3175–3182.
23. Shultz LD, Lyons BL, Burzenski LM, Gott B, Chen X, et al. (2005) Human lymphoid and myeloid cell development in NOD/LtSz-scid IL2R gamma null mice engrafted with mobilized human hemopoietic stem cells. *J Immunol* 174: 6477–6489.
24. Strowig T, Gurer C, Ploss A, Liu YF, Arrey F, et al. (2009) Priming of protective T cell responses against virus-induced tumors in mice with human immune system components. *J Exp Med* 206: 1423–1434.
25. Watanabe S, Terashima K, Ohta S, Horibata S, Yajima M, et al. (2007) Hematopoietic stem cell-engrafted NOD/SCID/IL2Rgamma null mice develop human lymphoid systems and induce long-lasting HIV-1 infection with specific humoral immune responses. *Blood* 109: 212–218.
26. Yajima M, Imadome K, Nakagawa A, Watanabe S, Terashima K, et al. (2008) A new humanized mouse model of Epstein-Barr virus infection that reproduces persistent infection, lymphoproliferative disorder, and cell-mediated and humoral immune responses. *J Infect Dis* 198: 673–682.
27. Traggiai E, Chicha L, Mazzucchelli L, Bronz L, Piffaretti JC, et al. (2004) Development of a human adaptive immune system in cord blood cell-transplanted mice. *Science* 304: 104–107.
28. Melkus MW, Estes JD, Padgett-Thomas A, Galin J, Denton PW, et al. (2006) Humanized mice mount specific adaptive and innate immune responses to EBV and TSST-1. *Nat Med* 12: 1316–1322.
29. Baenziger S, Tussiwand R, Schlaepfer E, Mazzucchelli L, Heikenwalder M, et al. (2006) Disseminated and sustained HIV infection in CD34+ cord blood cell-transplanted Rag2-/- gamma c-/- mice. *Proc Natl Acad Sci U S A* 103: 15951–15956.
30. Zhang L, Kovalev GI, Su L (2007) HIV-1 infection and pathogenesis in a novel humanized mouse model. *Blood* 109: 2978–2981.
31. Dewan MZ, Watanabe M, Ahmed S, Terashima K, Horiuchi S, et al. (2005) Hodgkin's lymphoma cells are efficiently engrafted and tumor marker CD30 is expressed with constitutive nuclear factor-kappaB activity in unconditioned NOD/SCID/gammac(null) mice. *Cancer Sci* 96: 466–473.
32. Ishikawa F, Yoshida S, Saito Y, Hijikata A, Kitamura H, et al. (2007) Chemotherapy-resistant human AML stem cells home to and engraft within the bone-marrow endosteal region. *Nat Biotechnol* 25: 1315–1321.
33. Durig J, Ebeling P, Grabellus F, Sorg UR, Mollmann M, et al. (2007) A novel nonobese diabetic/severe combined immunodeficient xenograft model for chronic lymphocytic leukemia reflects important clinical characteristics of the disease. *Cancer Res* 67: 8653–8661.
34. Nakagawa A, Ito M, Saga S (2002) Fatal cytotoxic T-cell proliferation in chronic active Epstein-Barr virus infection in childhood. *Am J Clin Pathol* 117: 283–290.
35. Nagata H, Konno A, Kimura N, Zhang Y, Kimura M, et al. (2001) Characterization of novel natural killer (NK)-cell and gammadelta T-cell lines established from primary lesions of nasal T/NK-cell lymphomas associated with the Epstein-Barr virus. *Blood* 97: 708–713.
36. Imai S, Sugiura M, Oikawa O, Koizumi S, Hirao M, et al. (1996) Epstein-Barr virus (EBV)-carrying and -expressing T-cell lines established from severe chronic active EBV infection. *Blood* 87: 1446–1457.
37. Yoshioka M, Ishiguro N, Ishiko H, Ma X, Kikuta H, et al. (2001) Heterogeneous, restricted patterns of Epstein-Barr virus (EBV) latent gene expression in patients with chronic active EBV infection. *J Gen Virol* 82: 2385–2392.
38. Kimura H, Hoshino Y, Hara S, Sugaya N, Kawada J, et al. (2005) Differences between T cell-type and natural killer cell-type chronic active Epstein-Barr virus infection. *J Infect Dis* 191: 531–539.
39. Xu J, Ahmad A, Jones JF, Dolcetti R, Vaccher E, et al. (2000) Elevated serum transforming growth factor beta1 levels in Epstein-Barr virus-associated diseases and their correlation with virus-specific immunoglobulin A (IgA) and IgM. *J Virol* 74: 2443–2446.
40. Ohga S, Nomura A, Takada H, Ihara K, Kawakami K, et al. (2001) Epstein-Barr virus (EBV) load and cytokine gene expression in activated T cells of chronic active EBV infection. *J Infect Dis* 183: 1–7.
41. Hayashi K, Ohara N, Teramoto N, Onoda S, Chen HL, et al. (2001) An animal model for human EBV-associated hemophagocytic syndrome: herpesvirus papio frequently induces fatal lymphoproliferative disorders with hemophagocytic syndrome in rabbits. *Am J Pathol* 158: 1533–1542.
42. Veronese ML, Veronesi A, D'Andrea E, Del Mistro A, Indraco S, et al. (1992) Lymphoproliferative disease in human peripheral blood mononuclear cell-injected SCID mice. I. T lymphocyte requirement for B cell tumor generation. *J Exp Med* 176: 1763–1767.
43. Johannessen I, Asghar M, Crawford DH (2000) Essential role for T cells in human B-cell lymphoproliferative disease development in severe combined immunodeficient mice. *Br J Haematol* 109: 600–610.
44. Sutkowski N, Palkama T, Ciurli C, Sekaly RP, Thorley-Lawson DA, et al. (1996) An Epstein-Barr virus-associated superantigen. *J Exp Med* 184: 971–980.
45. Anagnostopoulos I, Hummel M, Kreschel C, Stein H (1995) Morphology, immunophenotype, and distribution of latently and/or productively Epstein-Barr virus-infected cells in acute infectious mononucleosis: implications for the interindividual infection route of Epstein-Barr virus. *Blood* 85: 744–750.
46. Hudnall SD, Ge Y, Wei L, Yang NP, Wang HQ, et al. (2005) Distribution and phenotype of Epstein-Barr virus-infected cells in human pharyngeal tonsils. *Mod Pathol* 18: 519–527.
47. Hislop AD, Taylor GS, Sauce D, Rickinson AB (2007) Cellular responses to viral infection in humans: lessons from Epstein-Barr virus. *Annu Rev Immunol* 25: 587–617.
48. Katano H, Ali MA, Patera AC, Catalano M, Jaffe ES, et al. (2004) Chronic active Epstein-Barr virus infection associated with mutations in perforin that impair its maturation. *Blood* 103: 1244–1252.
49. van Rijn RS, Simonetti ER, Hagenbeek A, Hogenes MC, de Weger RA, et al. (2003) A new xenograft model for graft-versus-host disease by intravenous transfer of human peripheral blood mononuclear cells in RAG2-/- gammac-/- double-mutant mice. *Blood* 102: 2522–2531.
50. Ito R, Katano I, Kawai K, Hirata H, Ogura T, et al. (2009) Highly sensitive model for xenogenic GVHD using severe immunodeficient NOG mice. *Transplantation* 87: 1654–1658.
51. Kawa K, Sawada A, Sato M, Okamura T, Sakata N, et al. (2011) Excellent outcome of allogeneic hematopoietic SCT with reduced-intensity conditioning for the treatment of chronic active EBV infection. *Bone Marrow Transplant* 46: 77–83.
52. Sato E, Ohga S, Kuroda H, Yoshida F, Nishimura M, et al. (2008) Allogeneic hematopoietic stem cell transplantation for Epstein-Barr virus-associated T/natural killer-cell lymphoproliferative disease in Japan. *Am J Hematol* 83: 721–727.
53. Okano M, Kawa K, Kimura H, Yachie A, Wakiguchi H, et al. (2005) Proposed guidelines for diagnosing chronic active Epstein-Barr virus infection. *Am J Hematol* 80: 64–69.
54. Kimura H, Morita M, Yabuta Y, Kuzushima K, Kato K, et al. (1999) Quantitative analysis of Epstein-Barr virus load by using a real-time PCR assay. *J Clin Microbiol* 37: 132–136.
55. Nakamura H, Iwakiri D, Ono Y, Fujiwara S (1998) Epstein-Barr-virus-infected human T-cell line with a unique pattern of viral-gene expression. *Int J Cancer* 76: 587–594.

Novel Postentry Inhibitor of Human Immunodeficiency Virus Type 1 Replication Screened by Yeast Membrane-Associated Two-Hybrid System[∇]

Emiko Urano,^{1,2} Noriko Kuramochi,³ Reiko Ichikawa,² Somay Yamagata Murayama,¹
Kosuke Miyauchi,² Hiroshi Tomoda,³ Yutaka Takebe,² Milan Nermut,⁴
Jun Komano,^{2,*} and Yuko Morikawa^{1*}

Kitasato Institute for Life Sciences and Graduate School of Infection Control, Kitasato University, Shirokane 5-9-1, Minato-ku, Tokyo 108-8641, Japan¹; AIDS Research Center, National Institute of Infectious Diseases, Toyama 1-23-1, Shinjuku-ku, Tokyo 162-8640, Japan²; Faculty of Pharmaceutical Sciences, Kitasato University, Shirokane 5-9-1, Minato-ku, Tokyo 108-8641, Japan³; and National Institute for Biological Standards and Control, South Mimms, Herts EN6 3QG, United Kingdom⁴

Received 3 March 2011/Returned for modification 25 April 2011/Accepted 1 July 2011

Human immunodeficiency virus (HIV) Gag protein targets to the plasma membrane and assembles into viral particles. In the next round of infection, the mature Gag capsids disassemble during viral entry. Thus, Gag plays a central role in the HIV life cycle. Using a yeast membrane-associated two-hybrid assay based on the SOS-RAS signaling system, we developed a system to measure the Gag-Gag interaction and isolated 6 candidates for Gag assembly inhibitors from a chemical library composed of 20,000 small molecules. When tested in the human MT-4 cell line and primary peripheral blood mononuclear cells, one of the candidates, 2-(benzothiazol-2-ylmethylthio)-4-methylpyrimidine (BMMP), displayed an inhibitory effect on HIV replication, although a considerably high dose was required. Unexpectedly, neither particle production nor maturation was inhibited by BMMP. Confocal microscopy confirmed that BMMP did not block Gag plasma membrane targeting. Single-round infection assays with envelope-pseudotyped and luciferase-expressing viruses revealed that BMMP inhibited HIV replication postentry but not simian immunodeficiency virus (SIV) or murine leukemia virus infection. Studies with HIV/SIV Gag chimeras indicated that the Gag capsid (CA) domain was responsible for the BMMP-mediated HIV postentry block. *In vitro* studies indicated that BMMP accelerated disassembly of HIV cores and, conversely, inhibited assembly of purified CA protein in a dose-dependent manner. Collectively, our data suggest that BMMP primarily targets the HIV CA domain and disrupts viral infection postentry, possibly through inducing premature disassembly of HIV cores. We suggest that BMMP is a potential lead compound to develop antiretroviral drugs bearing novel mechanisms of action.

Over 2 decades, research has developed antiretroviral therapy (ART) with a combination of antiretroviral drugs for human immunodeficiency virus type 1 (HIV-1) infection (10). ART has dramatically improved the survival of HIV-1-infected individuals. Current ART involves a combination of inhibitors of HIV-specific enzymes, such as protease (PR), reverse transcriptase (RT), and integrase (IN). In some cases, inhibitors of HIV-1 entry are also used. However, the emergence of HIV-1 variants resistant to antiretroviral drugs during ART stresses the need for novel HIV-1 inhibitors against distinct targets.

Multiple screening approaches have been employed for HIV-1 drug discovery (37) and have successfully discovered HIV-1 inhibitors that are currently available: nucleoside analogue RT inhibitors were discovered by HIV replication assays (23) and PR inhibitors were produced by structure-based drug design (25). In general, cell-free assays allow discovery of com-

pounds with a relatively low 50% effective dose (ED₅₀) *in vitro*. However, many such compounds often fail to inhibit HIV-1 replication in *in vivo* assays, because they may not penetrate the cell membrane or may easily be catalyzed in metabolic environments. Also, possible toxic effects of the compounds must be tested in a subsequent cell culture study. In contrast, cell-based screens can exclude toxic compounds but have the disadvantages of time requirements and limitations on cell propagation in high-throughput screening.

Recently, cell-based assays using engineered cells and microorganisms have become an attractive alternative to *in vitro* assays for high-throughput screening. The yeast *Saccharomyces cerevisiae* is a convenient alternative to mammalian cells for this purpose. Comparative genomic analysis has shown that approximately 30% of yeast genes have homology to the mammalian protein sequences (8), indicating that basic cellular mechanisms are well conserved between yeast and human cells. Yeast has been used as a model organism for understanding biological functions of higher eukaryotic cells, leading to accumulation of scientific knowledge in yeast genetics and molecular biology. Such pioneering research has allowed the development of molecular technologies (e.g., two-hybrid assay and galactose induction), genetically modified cells (e.g., temperature sensitivity and conditional lethality), and cell selection systems (e.g.,

* Corresponding author. Mailing address for Jun Komano: AIDS Research Center, National Institute of Infectious Diseases, Toyama 1-23-1, Shinjuku-ku, Tokyo 162-8640, Japan. Phone: 81-3-5285-1111. Fax: 81-3-5282-5037. E-mail: ajkomano@nih.go.jp. Mailing address for Yuko Morikawa: Kitasato Institute for Life Sciences and Graduate School of Infection Control, Kitasato University, Shirokane 5-9-1, Minato-ku, Tokyo 108-8641, Japan. Phone: 81-3-3444-6161. Fax: 81-3-5791-6268. E-mail: morikawa@lisci.kitasato-u.ac.jp.

[∇] Published ahead of print on 11 July 2011.

URA3 nutritional selection), enabling the construction of simple readout assay systems.

Gag protein, the main structural component of retrovirus, directs particle assembly. HIV Gag protein is synthesized as a precursor protein, p55, which is composed of matrix (MA), capsid (CA), nucleocapsid (NC), and p6 domains, and cotranslationally myristoylated at the N-terminal glycine. Concomitant with the N-terminal myristoylation, p55Gag is targeted to the plasma membrane and assembled into virus particles (13, 22). During particle release, Gag undergoes proteolytic processing to generate the CA domain that forms the mature capsid. In the next round of infection, the mature capsid disassembles during viral penetration into host cell cytoplasm. Thus, the capsid assembly and disassembly are reverse reactions during virus release and entry and must be regulated by yet-unknown mechanisms. Indeed, the optimal stability of HIV-1 capsid is required for efficient infection (14). We have previously shown that the particle assembly process is reproducible in a yeast cell system (26). Here, we further developed a yeast membrane-associated two-hybrid assay system in which a temperature-sensitive mutant strain of yeast grows at restrictive temperature when Gag-Gag interactions occur. Using this yeast two-hybrid system, we have screened a chemical library composed of 20,000 low-molecular-weight compounds and have found a compound that targets CA-CA interactions and inhibits HIV-1 replication.

MATERIALS AND METHODS

Construction and transformation of yeast expression plasmids. A yeast membrane-associated two-hybrid assay based on the CytoTrap SOS recruitment system (Stratagene) was employed in this study. The full-length *gag* gene of HIV-1 (HXB2 strain) was placed downstream of the yeast inducible promoter for the *GAL1* gene in frame with the cDNA of SOS in a pSOS plasmid (Stratagene) that contains the *LEU2* gene as a yeast selective marker. The HIV-1 (HXB2 strain) *gag* gene was also cloned into pMyr plasmid, which contains a yeast inducible promoter for the *GAL1* gene and the *URA3* gene as a selective marker. The *S. cerevisiae* strain cdc25Ha (*MATa ura3-52 his3-200 ade2-101 lys2-801 trp1-901 leu2-3 112 cdc25-2 Gal⁺*) was doubly transformed with the yeast expression plasmids.

Chemical library screening in CytoTrap yeast membrane-associated two-hybrid system. Yeast transformants were initially grown at 25°C in synthetic defined medium with glucose (0.67% yeast nitrogen base, 2% glucose, and amino acid mixtures without uracil or leucine) (permissive conditions). After being washed, culture was diluted to an optical density at 600 nm (OD₆₀₀) of 0.1 in synthetic defined medium with galactose and raffinose (0.67% yeast nitrogen base, 2% galactose, 2% raffinose, and amino acid mixtures without uracil or leucine) for Gag expression. The yeast culture (OD₆₀₀ = 0.1) was incubated with a chemical library (a final concentration of 10 μM) at 37°C for 5 days (restrictive conditions) in 96-well microtiter plates with shaking. The chemical library (preplated Diversity Set) was purchased from Enamine. After complete resuspension of cells by vortexing of microtiter plates, cell density was measured at 600 nm by a plate reader (Infinite200; Tecan).

Mammalian cells and transfection. 293T, HeLa, and MT-4 cells were provided by the AIDS Research Center, National Institute of Infectious Diseases, Japan. 293FT cells were purchased from Invitrogen. Peripheral blood monocyte cells (PBMC) were isolated by Ficoll-Conray density centrifugation from healthy donors. All mammalian cells were maintained in RPMI 1640 medium (Sigma) supplemented with 10% fetal bovine serum (Japan Bioserum, Japan), 100 U/ml penicillin, and 100 mg/ml streptomycin (Invitrogen), at 37°C in a humidified 5% CO₂ atmosphere. For PBMC culture, GlutaMax-I (Invitrogen), insulin-transferin-selenium A (Invitrogen), 200 mg/ml anti-CD3 monoclonal antibody (OKT3; Janssen Pharmaceutical), and 70 U/ml recombinant human interleukin-2 (IL-2; Shionogi Pharmaceutical, Japan) were further added to the medium. Transfection was carried out with Lipofectamine 2000 according to the manufacturer's protocol (Invitrogen).

Cell toxicity assays. For determining the toxicity of the chemical library to yeast, yeast cultures were diluted to an OD₆₀₀ of 0.01 and incubated under permissive conditions (at 25°C in glucose medium) with the chemical library. After 2 days, cell density was measured at 600 nm by a plate reader (Infinite200; Tecan). For determining toxicity to mammalian cells, 293T, 293FT, HeLa, and MT-4 cells and PBMC were incubated with compounds at 37°C for 2 to 14 days and subjected to 3-(4,5-dimethylthiazol-2-yl)-5-(3-carboxymethoxyphenyl)-2-(4-sulfophenyl)-2H-tetrazolium (MTS) and Alamar Blue assays according to the manufacturer's instructions. The OD of the MTS assay mixture was measured at 490 nm, and the OD of the Alamar Blue assay mixture was measured at 570 nm by a plate reader (FLx800; BioTek). The 50% cytotoxicity concentrations were defined as drug concentrations by which the OD values reached the 50% level of the no-drug (dimethyl sulfoxide [DMSO]) controls.

HIV-1 replication assays. MT-4 Luc cells that were transduced with luciferase in MT-4 cells (31) and PBMC were grown in RPMI 1640 medium supplemented with 10% fetal bovine serum. MT-4 Luc cells were infected with HIV-1 (HXB2 strain) corresponding to 1.25 ng of p24CA antigen and incubated at 37°C in the presence of compounds. On day 7, MT-4 Luc cells were subjected to luciferase assay. PBMC were stimulated with IL-2 and anti-CD3 antibody. Following infection with HIV-1 (HXB2 strain) corresponding to approximately 5 ng of p24CA antigen, PBMC were incubated at 37°C and passaged every 3 to 4 days in the presence of compounds. The culture supernatants of PBMC were temporally collected and subjected to quantification of HIV-1 particle yields by p24CA antigen capture enzyme-linked immunosorbent assay (ELISA; Zeptometrix).

Single-round infection assays. For single-round infection assays, HIV-1 was pseudotyped with either HIV-1 Env protein or vesicular stomatitis virus (VSV) G protein as described previously (35). Briefly, 293FT cells were transfected with a plasmid containing the codon-optimized HXB2 *gag-pol* gene (pHIVgag-pol), a lentiviral plasmid expressing luciferase (pLenti-luciferase), a plasmid expressing HIV-1 Rev (pRevpac), and either a plasmid expressing HIV-1 Env or a plasmid expressing VSV-G. Culture media were harvested and inoculated into MT-4 and 293FT cells in the presence of 5 to 10 μg/ml dextran (ICN). HIV-1 pseudotyped with autologous HIV-1 Env protein was inoculated into 293FT-CD4 (expressing CD4 constitutively) cells. On day 2 or 3, infectivity was assessed by luciferase activity transduced by pLenti-luciferase. HIV-1 (NL43 strain) expressing luciferase, simian immunodeficiency virus (SIV) (mac239 strain), and murine leukemia virus (MLV) (Moloney strain) were similarly pseudotyped with VSV-G (28). The viruses were enriched by centrifugation through sucrose cushions if necessary.

HIV/SIV Gag chimeras were generated in the context of pHIVgag-pol by replacing the MA and CA domains with the SIV MA and CA domains, respectively. The Gag chimeras contain the cleavage site sequences of HIV-1 Gag at the chimera junctions. Amino acid substitutions G89A and P90A in the cyclophilin A (CypA)-binding loop of CA (corresponding to Gag amino acid positions 225 and 226) (11, 16) were carried out by overlap PCR in the context of pHIVgag-pol.

Quantitative PCR for HIV-1 cDNA synthesis. MT-4 cells were infected with HIV-1 (HXB2 strain) and incubated in the presence of compounds. Efavirenz (EFV) was provided by the NIH AIDS Research and Reference Reagent Program and was used as positive control. The cellular genomic DNA was extracted 4 and 24 h postinfection with a DNeasy kit (Qiagen) according to the manufacturer's instructions. The cellular DNA was subjected to quantitative real-time PCR using the Quantitec probe PCR kit containing SYBR green (Qiagen). The following primer sets were used: 5'-AACTAGGGAACCCACTGCTTAAG-3' and 5'-CTGCTAGAGATTTTCCACACTGAC-3' (specific for the R-U5 region in early reverse transcripts of HIV-1 cDNA), 5'-CCGTCTGTTGTGTGACTCTGGT-3' and 5'-GAGTCCCTGCGTTCGAGAGAGCT-3' (specific for the late reverse transcripts of HIV-1 cDNA), 5'-TGCTGGGATTACAGGCGTGAG-3' and 5'-CTGCTAGAGATTTTCCACACTGAC-3' (specific for long terminal repeat [LTR] and *Alu* region in the integrated HIV-1 cDNA), and 5'-AACTAGGGAACCCACTGCTTAAG-3' and 5'-CTGCTAGAGATTTTCCACACTGAC-3' (second PCR) (specific for LTR region in the integrated HIV-1 cDNA) (12). The amplification kinetics was monitored by the Opticon 2 system (BioRad). The levels of cellular DNA were normalized by the levels of β-globin DNA quantified using primers 5'-TATTGGTCTCCTTAAACCTGTCTTG-3' and 5'-CTGACACAACCTGTGTTCACTAGC-3' (19).

Viral protein expression and particle purification. HIV-1 proviral clone pHXB2 was transfected into 293FT and HeLa cells in the presence of increasing doses of 2-(benzothiazol-2-ylmethylthio)-4-methylpyrimidine (BMMP). After 2 days, cells were analyzed by Western blotting using anti-HIV-1 p24CA monoclonal antibody (100-fold diluent of 183-H12-5C hybridoma culture supernatant; NIH AIDS Research and Reference Reagent Program). HIV particles were collected by centrifugation through 20% (wt/vol) sucrose cushions in an SW55

rotor (Beckman Coulter) at $120,000 \times g$ for 1 h. For HIV/SIV Gag chimeras, 293FT cells were cotransfected with pHIVgag-pol expressing Gag chimera, pLenti-luciferase, pRevpac, and a plasmid expressing VSV-G. Cells and purified particles were similarly analyzed by Western blotting using anti-HIV-1 p24CA, anti-HIV-1 p17MA (2 $\mu\text{g/ml}$; 13-103-100; Advanced Biotechnologies), and anti-SIV p27CA (1 $\mu\text{g/ml}$; 4324; Advanced Bioscience Laboratories) monoclonal antibodies.

In vitro assembly reaction of CA. The *in vitro* assembly reaction of CA was performed as described previously (17, 36). Briefly, the purified HIV-1 CA (a final concentration of 100 μM) was incubated at 37°C for 1 h in buffer containing 20 mM Tris (pH 8.0), 500 mM NaCl, 0.2 mM EDTA, and 1 mM dithiothreitol. Assembly products were pelleted by centrifugation at $18,000 \times g$ for 30 min at 4°C and were subjected to p24CA antigen capture ELISA (Zeptomatrix) and electron microscopy.

In vitro disassembly reaction of capsid cores. The *in vitro* disassembly assay was performed according to Aiken's method with some modifications (3). HIV particles were purified by ultracentrifugation through 20% (wt/vol) sucrose cushions. For isolation of HIV capsid cores, purified HIV particles were applied onto sucrose step gradients composed of 7.5% (wt/vol), 15% (wt/vol) containing 1% Triton X-100, and 30 to 70% (wt/vol) sucrose and subjected to centrifugation at $120,000 \times g$ for 16 h at 4°C . Fractions rich in HIV cores were collected and resuspended in buffer (10 mM Tris [pH 7.4], 100 mM NaCl, and 1 mM EDTA). For core disassembly assays, aliquots of HIV cores were incubated at 37°C in the presence of compounds. For comparison, azidothymidine (AZT) (Moravak Biochemicals) was added to the reaction mixture. Intact cores were recovered by centrifugation at $125,000 \times g$ for 30 min at 4°C .

Confocal microscopy and electron microscopy. HeLa cells were transfected with a pNL43 derivative expressing Gag-green fluorescent protein (GFP) fusion protein but not *pol* gene products. Cells were fixed with 3.7% paraformaldehyde in phosphate-buffered saline (PBS) for 30 min at room temperature and were treated with 0.1% Triton X-100 for 10 min at room temperature for membrane permeabilization. Following nuclear staining with TO-PRO-3 (Molecular Probes), cells were mounted with antileaching reagent and observed with a laser scanning microscope (TCS; Leica).

In vitro assembly products were adsorbed onto carbon-coated copper grids and stained with 2% (wt/vol) uranyl acetate. Sections were subjected to electron microscopy.

Statistical analysis. Intergroup comparisons were performed with paired *t* test (for parametric group analysis). All *P* values were considered significant if less than 0.05.

RESULTS

A yeast membrane-associated two-hybrid system for HIV-1 Gag-Gag interactions. For construction of a yeast cell-based Gag assembly system, we employed a yeast membrane-associated two-hybrid assay based on the CytoTrap SOS recruitment system (Stratagene) in this study (Fig. 1). For HIV-1 Gag expression, two yeast expression plasmids, pMyr and pSOS, were used: pMyr contains the yeast inducible promoter for the *GAL1* gene followed by a myristoylation signal (amino acid sequence, MGSSKSKPKDPSQRR) for membrane targeting and pSOS contains the constitutive promoter for the yeast *ADH* gene followed by the human SOS gene. The *gag* gene of HIV-1 (HXB2 strain) was cloned in frame with the myristoylation signal in pMyr. The *gag* gene was similarly cloned in frame with the SOS gene in pSOS that allowed production of SOS-Gag fusion protein (Fig. 1A). The *S. cerevisiae* *cdc25H* strain was doubly transformed with these Gag expression plasmids. The *cdc25H* strain contains a temperature-sensitive mutation in the *CDC25* gene, which allows growth at 25°C (permissive temperature) but not at 37°C (restrictive temperature). SOS is the human orthologue of the yeast *CDC25* and can activate the yeast RAS signal transduction pathway that complements the yeast *cdc25* defect (4). When myristoylated Gag and SOS-Gag are coexpressed in the *cdc25H* cells, the SOS-Gag is recruited to the plasma membrane through an interac-

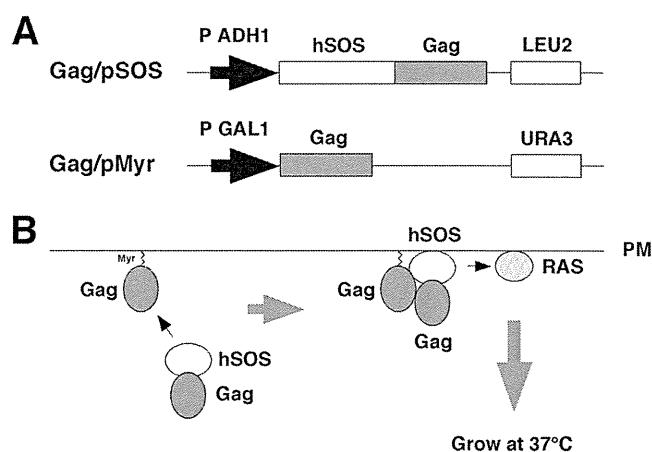


FIG. 1. Yeast membrane-associated two-hybrid screening for inhibitors of Gag-Gag interaction. (A) Schematic representation of Gag expression plasmids used for yeast SOS recruitment system. The full-length *gag* gene of HIV-1 (HXB2 strain) was expressed by yeast expression plasmids pMyr and pSOS: pMyr contains the yeast inducible promoter for the *GAL1* gene and the *URA3* gene as a selective marker and pSOS contains the constitutive promoter for the yeast *ADH* gene and the *LEU2* gene as a selective marker. (B) Principle of yeast membrane-associated two-hybrid assay based on SOS recruitment system. The schematic illustration was adapted with permission from the manuals for the CytoTrap yeast system (Agilent Technologies, Inc.; <http://www.genomics.agilent.com/CollectionSubpage.aspx?PageType=Product&SubPageType=ProductDetail&PageID=1311>).

tion with the myristoylated Gag, leading to growth of the *cdc25H* cells at 37°C (Fig. 1B). We initially confirmed that the *cdc25H* cells transformed with the Gag/pMyr and Gag/pSOS plasmids grew at 37°C in galactose plus raffinose medium under conditions in which SOS-Gag fusion protein was expressed but not at 37°C in glucose medium under conditions in which SOS-Gag fusion was not expressed.

Screening of a chemical library for Gag-Gag interaction inhibitors by yeast membrane-associated two-hybrid assays. For screening for inhibitors of Gag assembly, we optimized this yeast membrane-associated Gag-Gag interaction system to a liquid format using 96-well microplates. Using this system, we screened a chemical library composed of 20,000 compounds, each of which was initially designated by the numbers of microplates and wells of the chemical library (e.g., 172A6 indicates microplate number 172 and well number A6). When the *cdc25H* transformant was incubated at 37°C in galactose plus raffinose medium with a chemical library (10 μM each), we found 10 compounds that reduced cell growth (Fig. 2A, black columns). To examine if cell growth reduction is specifically due to the disruption of Gag-Gag interaction, we used another *cdc25H* transformant that contained MAFB/pSOS and SOS binding protein/pMyr plasmids. This combination produces SOS-MAFB fusion protein and myristoylated SOS binding protein and can be used as a positive control for the CytoTrap system (Stratagene). When using this positive control, we observed that 4 compounds (2G5, 73A7, 189A9, and 235C2) out of the 10 compounds also reduced cell growth (Fig. 2A, white columns), suggesting that they might inhibit pathways which are commonly used in the CytoTrap system (e.g., N myristoylation and RAS signaling). Thus, we concluded that 6 compounds (1G5, 31E7, 34A8, 73A5, 147B2, and 172A6) specifi-

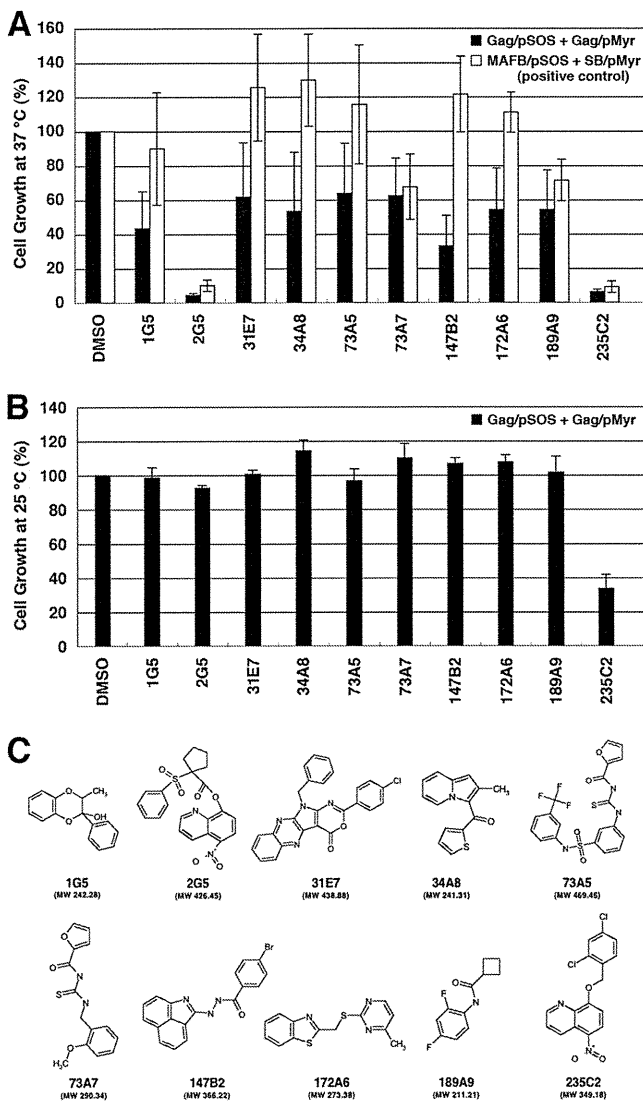


FIG. 2. Screening for inhibitors of Gag assembly by yeast membrane-associated two-hybrid assays. (A) The yeast *cdc25Ha* strain was transformed with the pSOS and pMyr plasmids. The yeast culture was diluted to an OD_{600} of 0.1 and incubated at 37°C in galactose-plus-raffinose medium (restrictive conditions) with a chemical library (a final concentration of 10 μ M). After growth at 37°C for 5 days, cell density was measured at OD_{600} . As a control, the OD_{600} of yeast incubated in the presence of DMSO was set to 100%. The yeast transformed with the pSOS and pMyr plasmids, both of which contained the HIV-1 *gag* gene, was shown as black columns, and the yeast was transformed with the pSOS plasmid containing MAFB and the pMyr plasmid containing the cDNA of SB (as a positive-control combination) as white columns. Data were shown as means with standard deviations from 5 independent experiments. (B) The yeast *cdc25Ha* strain transformed with the pSOS and pMyr plasmids containing the HIV-1 *gag* gene was grown at 25°C in glucose medium. The yeast culture was diluted to an OD_{600} of 0.01 and incubated at 25°C in glucose medium with a chemical library (a final concentration of 10 μ M). After growth at 25°C for 2 days, cell density was measured at OD_{600} . As a control, the OD_{600} of yeast incubated in the presence of DMSO was set to 100%. Data were shown as means with standard deviations from 3 independent experiments. (C) Structures of compounds screened from a chemical library by yeast membrane-associated two-hybrid assays.

cally inhibited a Gag-Gag interaction. No common chemical structures were found among the 6 candidates. However, 3 chemicals (34A8, 147B2, and 172A6) share relatively similar structures whereby two allyl groups are connected by a short linker moiety. To test the cell toxicity, the *cdc25H* transformants were incubated at 25°C in glucose medium (permissive conditions) with the compounds (10 μ M each) (Fig. 2B). All the compounds except 235C2 allowed cell growth at levels comparable to that obtained in the presence of DMSO (as a control). Further studies revealed that 235C2 preferentially inhibited growth of several fungi *in vitro* (e.g., *Candida albicans* and *Aspergillus fumigatus* at MICs of 5.7 and 10 μ M, respectively) (data not shown), suggesting that it might serve as a lead compound to develop an antifungal agent. The chemical formulas of 10 compounds are shown in Fig. 2C.

Inhibition of HIV replication in mammalian cells by compounds identified as yeast membrane-associated Gag-Gag interaction inhibitors. We evaluated the anti-HIV activity of the 6 candidates in mammalian cell systems. MT-4 Luc cells (human T lymphocytic cell line expressing luciferase constitutively) were infected with HIV-1 (HXB2 strain) and incubated at 37°C in the presence of the test compounds. In this T cell system, the luciferase activity is reduced by HIV-1 infection, due to the cell death upon HIV-1 replication (31). When added to HIV-1-infected MT-4 Luc cells, one of the candidates (172A6) recovered the luciferase expression in a dose-dependent manner (Fig. 3A), indicating that 172A6 was capable of reduction in HIV replication in mammalian cells. When 293T cells were incubated with the 6 compounds and were subjected to Alamar Blue assays, none of the compounds showed apparent reduction in cell viability (Fig. 3B). To confirm the anti-HIV effect, PBMC were infected with HIV-1 in the presence of 172A6 and production of HIV in the culture medium was temporally measured by p24CA antigen capture ELISA. 172A6 limited HIV replication at 5 μ M and severely inhibited it at 25 μ M (Fig. 3C, upper panel). When uninfected PBMC were similarly exposed to 172A6 and assessed by MTS assays, a slight reduction in cell viability was observed at 25 μ M (Fig. 3C, lower panel). However, the severe inhibition of HIV replication at 25 μ M 172A6 could not be ascribed fully to its cytotoxic effect. Using several mammalian cell lines, we reevaluated cytotoxicity of 172A6 by MTS assays. No significant cytotoxicity of 172A6 was seen in the cell lines, except in PBMC, that we used in this study (Fig. 3D). Based on the chemical structure [2-(benzothiazol-2-ylmethylthio)-4-methylpyrimidine] of the compound 172A6 (Fig. 2C), we called it BMMP here.

No inhibition of HIV particle release by BMMP. We initially examined whether BMMP inhibited HIV-1 particle production. 293FT cells were transfected with pHXB2 and incubated at 37°C in the presence of 5 to 50 μ M BMMP. Western blotting using anti-HIV-1 p24CA antibody revealed that the intracellular level of Gag expression and the pattern of Gag processing were largely unaffected in the presence of BMMP (Fig. 4A), suggesting that BMMP did not inhibit HIV protease. When purified particle fractions were similarly analyzed, we found no reduction in particle production (Fig. 4A). We obtained similar results on HeLa cells. This indicates that BMMP did not block HIV-1 particle release.

Intracellular distribution of Gag was examined by confocal